[UCI]I804:24011-200000366325

2021년 2월

박사학위 논문

Cloning and characterization of a recombinant metalloprotease rvFMP as a thrombolytic enzyme in human plasma and rat thrombosis models

조선대학교 대학원

글로벌바이오융합학과

임 도 성

Cloning and characterization of a recombinant metalloprotease rvFMP as a thrombolytic enzyme in human plasma and rat thrombosis models

인간 혈장 및 쥐 혈전증 모델에서 재조합 단백질분해효소 **rvFMP**의 혈전용해 특성에 관한 연구

2021년 **2**월 **25**일

조선대학교 대학원

글로벌바이오융합학과

임 도 성

Cloning and characterization of a recombinant metalloprotease rvFMP as a thrombolytic enzyme in human plasma and rat thrombosis models

지도교수 이 정 섭

이 논문을 이학 박사학위 신청 논문으로 제출함.

2020년 10월

조선대학교 대학원

글로벌바이오융합학과

임 도 성

임도성의 박사학위논문을 인준함.

위원장	조선대학교	교수	윤 성 명	(인)
위 원	원광대학교	교수	박 종 군	(인)
위 원	조선대학교	교수	이 건 호	(인)
위 원	조선대학교	교수	김 석 준	(인)
위 원	조선대학교	교수	이 정 섭	(인)

2020년 12월

조선대학교 대학원

CONTENTS

LIST OF TABLES

LIST OF FIGURES

ABBREVIATIONS

1,10-PT	1,10-phenanthroline
ATIII	Anti-thrombin III
BSA	Bovine serum albumin
CAPS	3-(cyclohexylamino)-1-propanesulfonic acid
DFP	Diisopropyl fluorophosphate
DTT	Dithiothreitol
EDTA	Ethylenediamine tetraacetic acid
ELISA	Enzyme-linked immunosorbent assay
EtBr	Ethidium bromide
FV	Factor V
FVII	Factor VII
FVIII	Factor VIII
FIX	Factor IX
FX	Factor X
FXI	Factor XI
FXII	Factor XII
FXIII	Factor XIII
GSP	Gene specific primer
HMWK	High molecular weight kininogen
HRP	Horseradish peroxidase
IPTG	Isopropyl-1-thio-β-d-galactopyranoside
LB	Luria-Bertani medium
PBS	Phosphate buffered saline
PAGE	Polyacrylamide gel electrophoresis
PAI	Plasminogen activator inhibitor
PCR	Polymerase chain reaction

PEG	Polyethylene glycol
PPK	Prekallikrein
PMSF	Phenylmethanesulfonyl fluoride
*p*NA	*p*-nitroanilide
RT	Room temperature
rvFMP	recombinant *Vibrio furnissii* metalloprotease
SD	Sprague-Dawley
SDS	Sodium dodecyl sulfate
TBS	Tris-buffer saline
TCA	Trichloroacetic acid
TF	Tissue factor
TFPI	Tissue factor pathway inhibitor
TLCK	Tosyl-lysine chloromethyl ketone
TPCK	Tosyl-phenylalanyl chloromethyl ketone
tPA	Tissue-type plasminogen activator
uPA	Urokinase-type plasminogen activator
TMB	Tetramethylbenzidine
TNF-α	Tumour necrosis factor-α
TT	Thrombin time

ABSTRACT

Cloning and characterization of a recombinant metalloprotease rvFMP as a thrombolytic enzyme in human plasma and rat thrombosis models

Do Sung Lim
Advisor : Prof. Jung Sup Lee, Ph.D.
Department of Integrative Biological Sciences
Graduate School of Chosun University

Cardiovascular diseases are the number one cause of death worldwide, which can be mainly induced by the fibrin deposits remained in arteries. Although several enzymes, including urokinase (uPA), streptokinase, and tissue-type plasminogen activator (tPA) are currently being used for a thrombolytic medication, they are all indirect enzymes activating plasminogen to plasmin that actually cleaves fibrin clots deposited in a blood vessel. However, the plasminogen activators show side effects such as bleeding, low blood pressure, nausea, and allergic reactions. This study was performed to develop a novel recombinant thrombolytic enzyme that can directly digest fibrin clots from *Vibrio furnissii* , a free-living marine bacterium that can be associated with gastroenteritis and skin lesions. There has been no report on extracellular protease(s) from *V. furnissii* in terms of developing a thrombolytic agent. This bacterium produces an extracellular 44 kDa metalloprotease named vFMP

(stands for *V. furnissii* metalloprotease) as found by this laboratory. In this study, a vFMP-encoding gene was cloned from the genomic DNA of *V. furnissii* strain KCCM41679 using polymerase chain reaction (PCR) and expressed in *Escherichia coli*, from which a recombinant vFMP (named rvFMP; stands for recombinant *V. furnissii* metalloprotease) was purified and characterized. The sequencing data (deposited in the GenBank database under an accession number MG954380) showed that the vFMP-encoding gene contains an open reading frame (ORF) composed of 1,827 nucleotides, which can encode 608 amino acids with a predicted molecular mass of 67443.71 Da. The start and stop codons of the cloned gene were found to be ATG and TAA, respectively. When the deduced amino acid sequence of the cloned gene was compared with those of five other *Vibrio*-derived proteases from *V. fluvialis* (WP_020431607.1), *Vibrio* sp. RC586 (EEY99547.1), *V. anguillarum* (AAM15681.1), *V. mimicus* (BAG30958.1), and *V. vulnificus* (ALM73800.1) (number in parenthesis indicates GenBank accession number), there was an average of approximately 80.8% sequence similarity between their mature peptide regions. These results suggest that they are highly conserved proteases. The sequence comparison data also showed that the cloned gene can produce a prepro-rvFMP composed of 608 amino acids, which is organized with a signal peptide (24 amino acids), an N-terminal propeptide (173 amino acids), and a catalytic domain (411 amino acids) containing a typical Zn^{2+}-binding motif (HEXXHG-X_{18}-E) that is often found from other bacterial metalloproteases. The recombinant vFMP enzyme (rvFMP) expressed in *E. coli* was purified using two anion chromatographic steps employing HiTrap Q FF and Source 15 Q 4.6/100 PE columns and an additional size exclusion chromatography with Superdex 75 10/300 GL

gel in order. The molecular masses of the purified enzymes were found to be approximately 44 kDa (processed form) and 39 kDa (truncated form) as determined by sodium dodecyl sulfate polyacrylamide gel electrophoresis (SDS-PAGE). The optimal pH and temperature for the rvFMP activity were found to be 7.0 and 50°C, respectively, when azocasein was used as a substrate. The proteolytic activity of rvFMP could be inhibited by typical metalloprotease inhibitors such as ethylenediaminetetraacetic acid (EDTA) and 1,10-phenanthroline (1,10-PT), but not by serine protease inhibitors, including phenylmethylsulfonyl fluoride (PMSF) and diisopropyl fluorophosphate (DFP). These results suggest that rvFMP is a typical metalloprotease. The purified protease was able to cleave various plasma proteins, including BSA, fibrinogen, prothrombin, collagen type IV, and plasminogen. The putative proteolytic cleavage site of rvFMP was a peptide bond located in the amino side of valine, as judged by N-terminal sequencing with two-digests of fibrinogen. The rvFMP enzyme showed fibrinogenolytic and fibrinolytic activities, as determined by *in vitro* cleavage assay. rvFMP could cleave all chains of fibrinogen, in which the Aα and B β chains could be digested completely within 1 min with a mass ratio of 1:7.9 (enzyme *vs* fibrinogen). The turbidity assay also showed that the relative turbidity of the fibrin polymer was decreased with plasmin (used as a positive control) or rvFMP treatment in a time-dependent manner. These results suggest that rvFMP has an enzyme activity to digest fibrin polymer actively. In addition, rvFMP could cleave cross-linked fibrin (XL-fibrin), as shown by SDS-PAGE and fibrin plate assay. In particular, plasmin (2 μg) and rvFMP (2 μg) could form clear halo-zones with diameters of 0.7 cm and 1.1cm, respectively, on fibrin plate. These results suggest that rvFMP has a clear XL-fibrin cleavage activity, approximately 2.5 times stronger

than the same amount of plasmin *in vitro*. In this study, the *in vivo* anti-thrombotic effect of rvFMP on vascular thrombosis induced by $FeCl_3$ exposure in rat carotid artery or kappa-carrageenan treatment in rat tail was also examined. Phosphate buffered saline (PBS), uPA (5.24 mg/kg), or rvFMP alone (100 μg/kg) showed no effect on the induction of the thrombus formation in the rat carotid artery, whereas the exposure of $FeCl_3$ resulted in an extensive arterial thrombosis as expected. However, the formation of thrombi by the exposure of $FeCl_3$ could be clearly reduced in a dose-dependent manner, when various doses of rvFMP (10-100 μg/kg) were pre-injected. This anti-thrombotic activity of rvFMP was also confirmed with the kappa-carrageenan-induced rat tail thrombosis model. The formation of vascular thrombi caused by 4 mg/kg of the carrageenan was clearly and dose-dependently decreased by the administration of uPA (5.24 mg/kg) or various concentrations of rvFMP (25-100 μg/kg). All these results suggest that rvFMP can digest effectively vascular thrombi *in vivo*. It was also revealed that rvFMP (1.5 mg/kg) evokes no internal bleeding and plasma fibrinogen depletion significantly, with no lethal effect on mice. In addition, the recombinant enzyme also showed no cytotoxicity and could not evoke the production of a typical inflammatory cytokine, tumour necrosis factor-α (TNF-α) in Raw 264.7 cells. Taken together, all these results demonstrate that rvFMP can be a candidate protease capable of being developed as a novel direct-acting thrombolytic agent.

1. INTRODUCTION

Blood hemostasis is a physiological system that stops bleeding and keeps blood in damaged blood vessels (Clemetson *et al.,* 2012). This system maintains the cardiovascular, digestive, respiratory, endocrine, and other systems essential and functionally (Marieb *et al.,* 2010). A normal hemostatic system inhibits thrombosis in the bloodstream but prevents bleeding in response to vascular damage. Blood constancy is maintained by the balance between fibrin formation and decomposition (Fig. 1). According to a recent report by the World Health Organization (WHO, 2016), cardiovascular disease (CVD) are the number one cause of death globally: more people die annually from CVDs than from any other cause. An estimated 17.9 million people died from CVDs in 2016, representing 31% of all global deaths. Of these deaths, approximately 85% are due to heart attack and stroke (WHO, 2016). Heart attacks and strokes are usually acute events and are mostly caused by blockages that prevent blood from flowing to the heart or brain. The most common reason for this is the accumulation of fat in the lining of the blood vessels that supply the heart or brain. A stroke can also be caused by bleeding from blood vessels or blood clots in the brain. Intravascular thrombosis, the formation of a clot of blood in a blood vessel, is one of the main causes of various CVDs (WHO, 2016). The major protein component of fibrin clots is formed from fibrinogen via thrombin-mediated proteolysis (Goldhaber *et al*., 2001).

However, the fibrin clots can be hydrolyzed by plasmin to remove thrombosis from blood vessels. In some situations, there is an imbalance due to some disorders and not hydrolyzed clots, resulting in thrombosis (Tough *et al*., 2005). Over the years, thrombolytic therapies like injecting or orally administrating thrombolytic agents to lyse thrombi in blood vessels have been

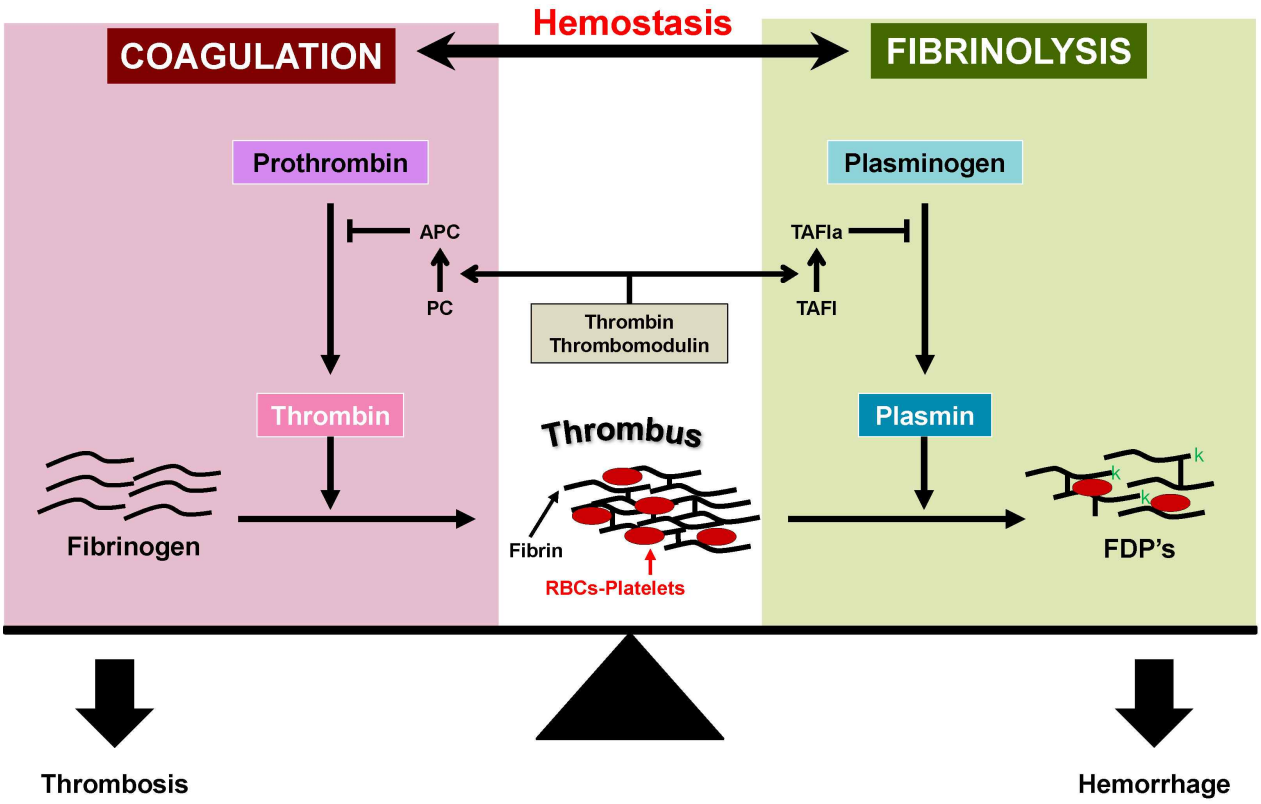

Correspondence, Niraj & Mishra, Niraj. (2012). Antithrombotic therapy: current status and future developments. theHealth. 3. 98-108.

Fig. 1. The balance between coagulation and fibrinolysis. The coagulation cascade ultimately generates thrombin, which catalyzes the conversion of fibrinogen to the fibrin clot. The fibrinolytic cascade generates plasmin, which catalyzes solubilization of the Fibrin. The thrombin-thrombomodulin complex promotes down-regulation of thrombin formation by generating activated protein C (APC). It also suppresses fibrinolysis by forming TAFIa. The two cascades are thereby linked through the thrombin, thrombomodulin, and TAFI pathway.

extensively investigated (Peng *et al.,* 2005). However, blood clots formed in blood vessels can interfere with blood flow through the circulatory system. When blood vessels are damaged, the body uses platelets and fibre to form blood clots to prevent blood loss (Marieb *et al.,* 2010). A clot that is freely looted and begins to move around the body is called an embolus (Boon *et al.,* 1993). A heart attack or stroke may occur when an area of plaque ruptures and a clot forms over the location, blocking the flow of blood to the organ's tissues. Deep vein thrombosis is a condition where blood clots develop usually in the deep veins of the legs. Pulmonary embolus occurs when these clots break away from the walls of the vein and travel to the pulmonary arteries supplying to the lungs through the heart (Lippi *et al.,* 2013). The formation of a thrombus is a dependent on both the activation of platelets, leading to platelet aggregation, and the activation of the coagulation cascade, leading to fibrin formation (Lippi *et al.,* 2013; Pancioli *et al.,* 2009). In recent years, many researchers have developed many anticoagulants and fibre-soluble enzymes to treat thrombosis. Anticoagulants can reduce the ability of the blood to clot (Blann *et al.,* 2002; Perler *et al.,* 2005). These remedial agents were developed after discovering the mechanisms of blood coagulation and fibrinolysis.

Blood coagulation cascades are divided into external (also called tissue factors) and intrinsic (also known as contact activation). The beginning of both paths leads to the activation of factor X (FX), which induces thrombin formation, which is called a common path (Nesheim *et al.,* 2003) (Fig. 2). In extrinsic pathways, vascular damage and exposure to tissue factors (TFs) can lead to platelets or endothelial cell activation. TFs combine coagulation factor VII (FVII) to initiate the formation of TF-FVII enabled complex. The TF-FVIIa complex can activate factor IX (FIX) through protein decomposition. Activated FIX (FIXa) may also activate FX with the presence of an active secondary factor VIII (FVIIIa)

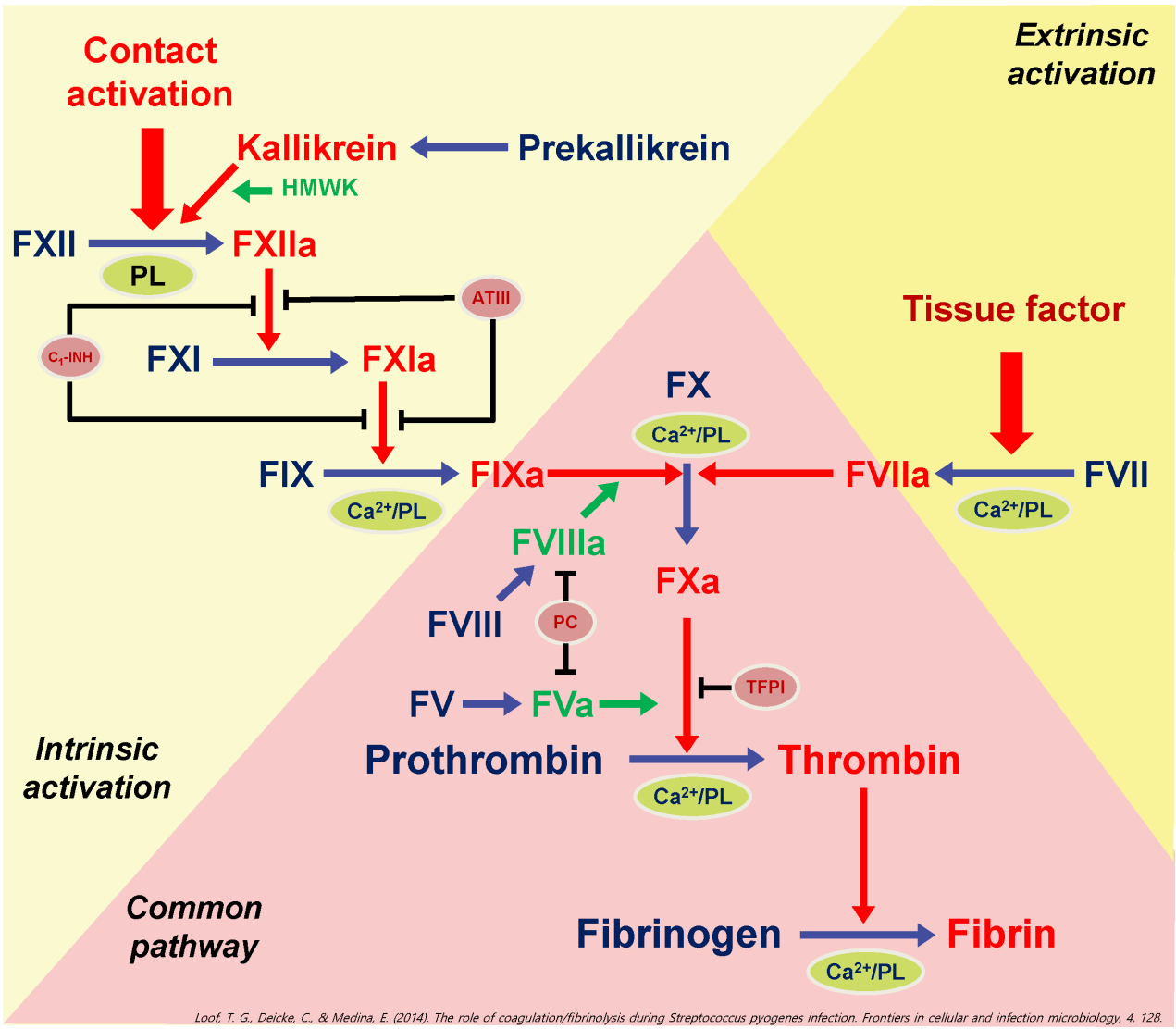

Fig. 2. Blood coagulation cascade. Two pathways lead to the formation of a fibrin clot: the intrinsic and the extrinsic pathway. The extrinsic pathway is the response to tissue injury, meanwhile the intrinsic pathway is the response to an abnormal vessel wall. Although they are initiated by distinct mechanisms, the two converge on a common pathway that leads to clot formation.

(Hoffman and Monroe, 2007) (Fig. 2). Factor XII triggers the intrinsic pathway (FXII, also called Hageman factor) when it contacts with a negatively charged surface such as glass or membrane of an activated platelet, provided the prekallikrein and its cofactor with high molecular weight kininogen (HMWK) (Hoffman and Monroe, 2007). Activated FXII (FXIIa) proteolytically cleaved factor XI (FXI) and then factor IX is activated by the FXIa (Riddel *et al*., 2007; Tanaka *et al*., 2009) (Fig. 2). The common pathway is initiated by activation of FX by either intrinsic or extrinsic pathways. Circulating activated factor VII (VIIa) combined with tissue factor (TF) derived from damaged tissues or expressed on activated monocytes (Fig. 2). In the presence of tissue factor, VIIa provides a potent stimulus for the activation of factor X to Xa. This pathway initiates physiologic hemostasis, generating small amounts of thrombin, which then feeds back to activate the intrinsic coagulation factors and subsequently generate higher thrombin levels. Then it catalyzes the proteolysis of the soluble plasma protein fibrinogen to fibrin. The fibrin monomers polymerize to form insoluble fibrin (Carter Angela *et al.,* 2007). In the cascade's final step, soluble fibrinogen is converted to insoluble fibrin by a serine protease called thrombin. The resulting fibrin monomers are spontaneously polymerized into cross-linked fibrin fibre in the presence of fibrin stabilizing factor FXIIIa (Carter Angela *et al.,* 2007).

Fibrinogen and fibrin play essential roles in blood clotting, wound healing, cell-to-cell interactions, and inflammatory responses (Jennewein *et al*., 2011) (Fig. 3A). As shown in Fig. 3A, the fibrinogen is composed of six polypeptide chains: two each of Aα, Bβ, and γ, joined by disulfide bonds and the dimeric structure can be categorized into four major domains: central E domain, two identical terminal D domain, and coiled-coil C domain (Mosesson *et al*., 2005). The N-terminus of the central E domain is composed of the fibrinopeptides A

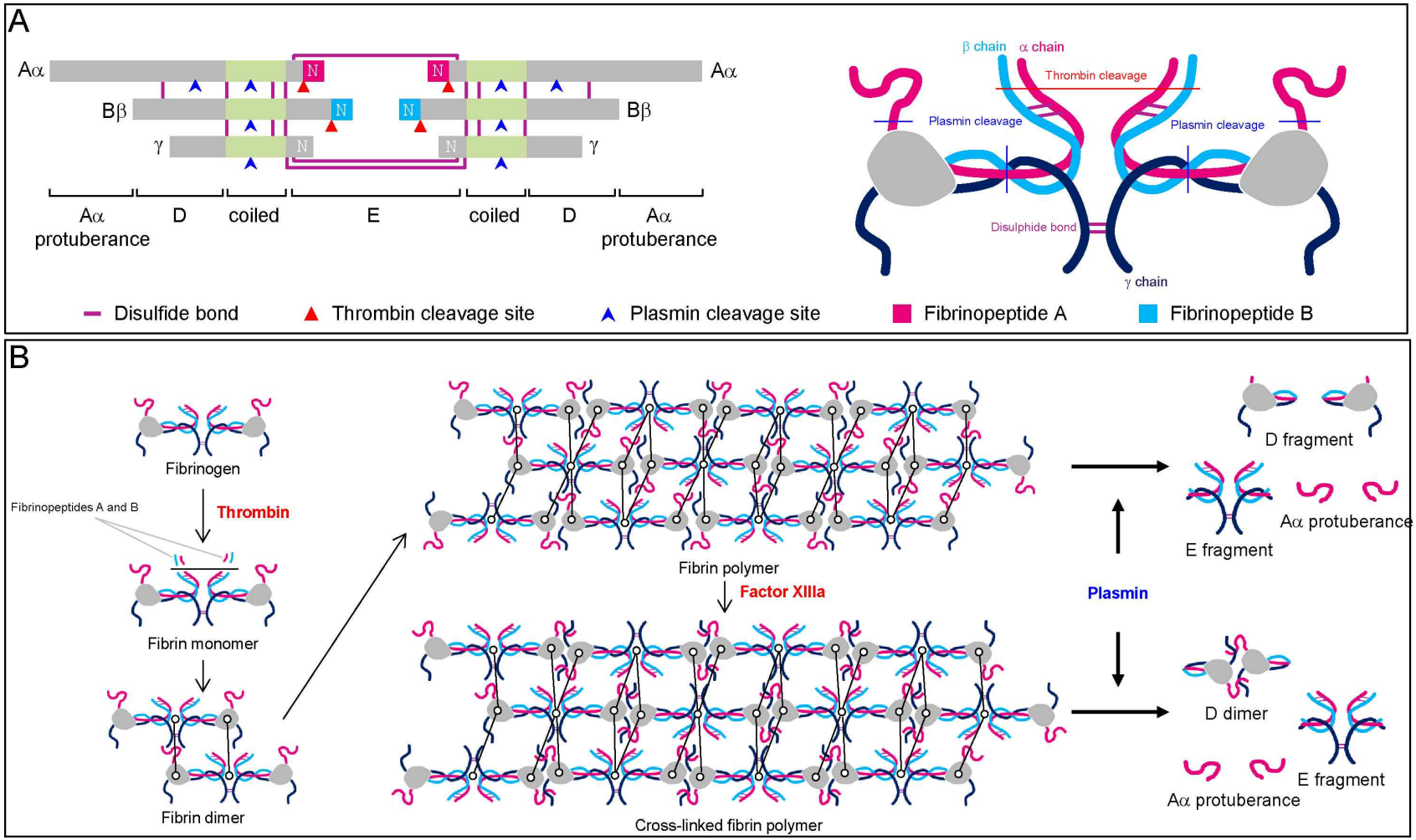

Fig. 3. The conversion of fibrinogen to fibrin. (A) The polypeptide and domain composition of fibrinogen. (B) Pathway of fibrin polymerization and degradation.

and B. During the coagulation process (Fig. 3B), the conversion of fibrinogen to fibrin occurs after the removal of fibrinopeptides A (FPA) and B (FPB) by thrombin from the N-termini of the Aα and Bβ chains (Mosesson *et al*., 2005). The fibrin monomers devoid of the fibrinopeptides have (αβγ)2 structures and then exposed the polymerization site of E domain that interacts to D domain of fibrin monomer (Mosesson *et al*., 2005). Fibrin polymer continues to make entangled long fibres, the fibrin clot. In the presence of FXIIIa, the fibrin clot is stabilized to form γ-γ dimer and α-α polymers (Mosesson *et al*., 2005). These cross-links help strengthen the fibrin clot, making it more resistant to physical and chemical damage (Mosesson *et al*., 2005). The fibrin deposits formed in arteries cause an intravascular thrombosis, which can induce cardiovascular diseases, such as myocardial infarction (Acharya and Dimichele, 2008). Therefore, fibrin clots formed eventually should be broken down into soluble peptides to be removed from the vessel, in which an endogenous serine protease, plasmin is directly involved (Lippi *et al.,* 2013; Pancioli *et al.,* 2009; Ghosh *et al*., 2012; Sakuragawa *et al*., 1975). Fibrin formation from fibrinogen is summarized in Fig. 3B.

The fibrin clotting is subsequently digested by the fibrinolytic system (Fig. 4). The enzyme plasmin is proteolytically generated from the zymogen called plasminogen by plasminogen activators (PAs), such as tissue-type plasminogen activator (tPA) and urokinase-type plasminogen activator (uPA) (Collen *et al*., 1986). Plasmin is activated by itself in plasminogen by the production of uPA and tPA. However, the conversion of uPA and tPA is regulated by plasminogen activation inhibitors -1 and -2 (PAI1 and PAI2). Furthermore, activated plasmin is inhibited by α2-antiplasmin and α2-macroglobulin (Shanmukhappa *et al*., 2005) (Fig. 4).

Several types of PAs derived from tPA and uPA are currently being used

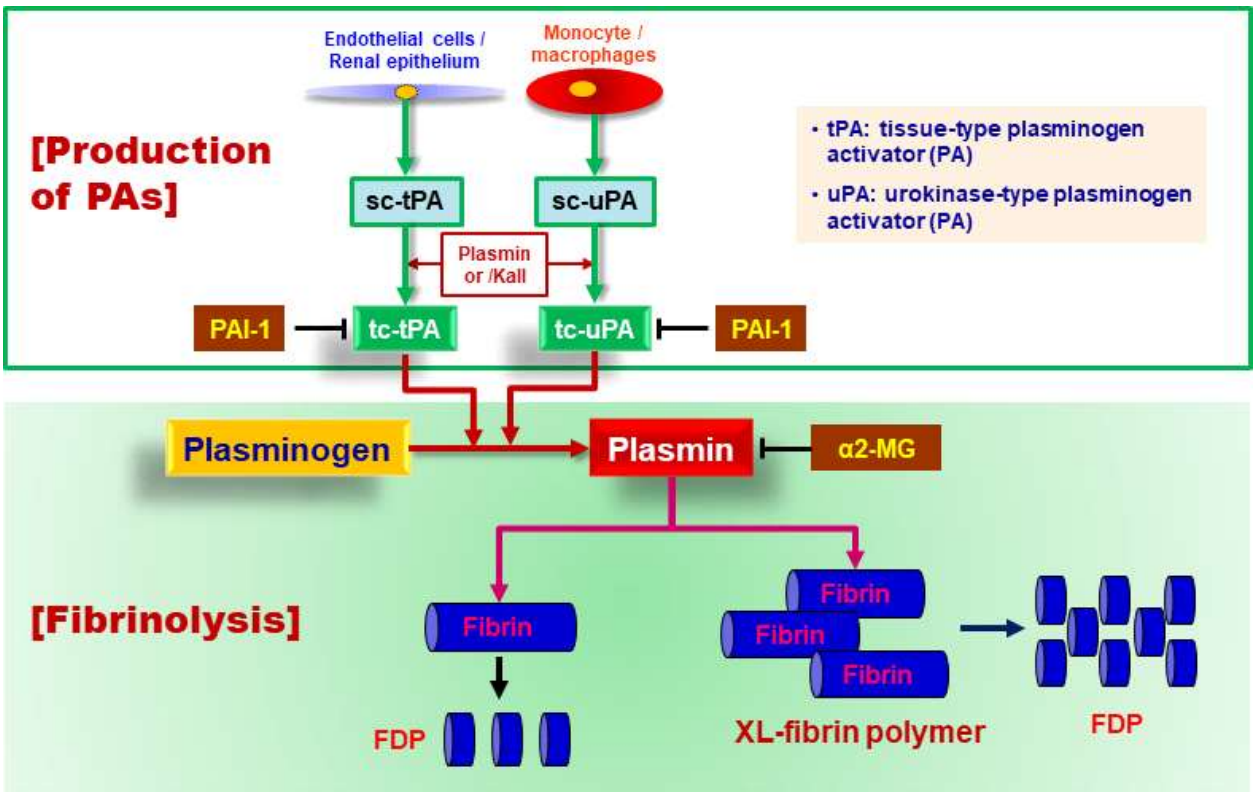

Fig. 4. Overview of the fibrinolytic system. Plasminogen activators, such as tissue plasminogen activator (tPA) or urokinase, activate plasminogen to form plasmin. Plasmin enzymatically cleaves insoluble fibrin polymers into soluble degradation products (FDP), thereby effecting the removal of unnecessary fibrin clot.

clinically as therapeutic agents to dissolve the fibrin deposits in the blood vessels (Ghosh *et al*., 2012). However, they are all indirect thrombolytic enzymes because the enzymes are acting as just activators for plasminogen to yield plasmin (Ghosh *et al*., 2012; Sakuragawa *et al*., 1975; Collen *et al*., 1986; Verstraete *et al*., 2000) (Tables 1 and 2). Moreover, they have a limitation in use due to their risks of bleeding complication, including intracranial haemorrhage, low fibrin specificity resulted from “plasminogen steal”, a short half-life, and immunogenicity resulting in drug resistance, fever, and allergic reactions (Ghosh *et al*., 2012; Verstraete *et al*., 2000; Arnold *et al*., 1995). These are the reasons why novel thrombolytic agents that can directly act on fibrin clots to cleave and also show no or significantly alleviated side effects should still be screened and developed from various sources. To date, many fibrin(ogen)olytic enzymes have been purified and characterized from snake venoms (De-Simone *et al*., 2005; Leonardi *et al*., 2002), marine green algae (Matsubara *et al*., 2000; Amarant *et al*., 1991; Matsushima *et al*., 1993), earthworm (Akazawa *et al*., 2018), and polychaete worms (Park *et al*., 2013). However, a safe, inexpensive, and effective direct-acting thrombolytic enzyme has not yet been developed.

Vibrio furnissii is a free-living marine bacterium. It is ubiquitously present in marine environments and is one of the 11 non-cholera vibrio species pathogenic in humans, which can lead to human gastroenteritis and extra-intestinal manifestations (Brenner *et al.,* 1983; Derber *et al.,* 2011; Ballal *et al.,* 2017), and its whole genome sequence has been determined in 2011 (Lux *et al.,* 2011). It produces a variety of secondary metabolites such as ectoine and bacteriocin that can be used as an active ingredient in skin care for sunlight protection, a replacement for antibiotics, and food preservative (Giubergia *et al.,* 2016). In addition, several Vibrio strains are known to secrete a variety of

Table 1. Thrombolytic agents currently being used in clinic.

Product name	Origin	Company	Country	Features & Side effects
Alteplase® TNKase® (rt-PA)	Human tPA produced by recombinant DNA technology	Genetech, Inc.	USA	• Fibrinolytic through plasminogen activation • Medical (vascular injection) • Recombinant protein
Abbokinase® (Urokinase)	Human neonatal kidney cells grown in tissue culture	Abbott Laboratories	USA	• Fibrinolytic through plasminogen activation • Bleeding and hypersensitivity reactions • Medical (vascular injection)
Streptase® (Streptokinase, SK)	Group C (beta) –hemolytic *Streptococci*	Aventis	France	• Fibrinolytic through plasminogen activation • Bleeding and hypersensitivity reactions • Antigen-acting antibody formation
Urokinase	Human urine	Green Cross	Korea	• Fibrinolytic through plasminogen activation • Bleeding and hypersensitivity reactions • Medical (vascular injection)
Mucolase Tab. (Streptokinase)	Group C hemolytic *Streptococci*	Hanmi Pharm. Co.	Korea	• Bleeding and hypersensitivity reactions • Antigen-acting antibody formation • Medical (oral administration)
Lumbriko Gold (Lumbrokinase)	*Lumbricusrubellus* (blood worm)	Lumbriko World, Inc.	USA	• Health supplements (blood circulation improvement) • Includes thrombolytic enzyme
Boluoke® (Lumbrokinase)	*Lumbricusrubellus* (blood worm)	Canada RNA Biochemical, Inc.	Canada	• Health supplements (blood circulation improvement) • Includes thrombolytic enzyme
Lumbrokinase	*Lumbricusrubellus* (blood worm)	Allergy Research Group	China	• Health supplements (blood circulation improvement) • Includes thrombolytic enzyme
Nattokinase NSK-SD®	Natto (*Bacillus subtilis* sub sp. Natto)	Allergy Research Group	China	• Health supplements (blood circulation improvement) • Includes thrombolytic enzyme

Table 2. Representative thrombolytic enzymes and blood circulation improving agents.

Product name	Origin	Company	Country	Features & Side effects
Urokinase	Human tPA produced by recombinant DNA technology	Genetech, Inc.	USA	• Fibrinolytic through plasminogen activation • Bleeding and hypersensitivity reactions • Medical (vascular injection)
Mucolase Tab.(Streptokinase &Streptodornase)	Human neonatal kidney cells grown in tissue culture	Abbott Laboratories	USA	• Relieving symptoms of sinusitis and thrombophlebitis • Bleeding and hypersensitivity reactions • Antigen-acting antibody formation • Medical (Oral administration)
Natto NKCP	Natto (*Bacillus subtilis* sub sp. Natto)	IL-YANG PHARM.	Japan	• Health supplements (blood circulation improvement) • Includes thrombolytic enzyme
MegaNattokinase	Natto (*Bacillus subtilis* sub sp. Natto)	CKD Healthcare	Japan	• Health supplements (blood circulation improvement) • Includes thrombolytic enzyme
Natokinase Gold	Natto (*Bacillus subtilis* sub sp. Natto)	Kyung Nam Pharm	Korea	• Health supplements (blood circulation improvement) • Includes thrombolytic enzyme

proteases that can cleave fibrinogen and fibrin. They include vEP-45 from *V. vulnificus* ATCC29307 (Chang *et al.*, 2005), vEP-MO6 from *V. vulnificus,* MO6 24/0 (Kwon *et al.,* 2007), and AKP-Vm from *V. metschnikovii* (Park *et al.,* 2012). This means that there may be a chance to find enzymes that can directly and effectively degrade blood clots. However, there is no report on any extracellular protease from *V. furnissii* in terms of the development of a thrombolytic agent.

In this study, a metalloprotease vFMP-encoding gene was cloned from the genomic DNA of *V. furnissii* KCCM41679, sequenced, and expressed in *Escherichia coli*. The recombinant vFMP (named rvFMP; stands for recombinant *V. furnissii* metalloprotease) expressed was purified using several chromatographic steps and its biochemical properties were characterized in terms of in vitro fibrin(ogen)olytic activity and in vivo thrombolytic ability in two kinds of rat thrombosis models.

2. MATERIALS AND METHODS

2-1. Bacterial strains and materials

Vibrio furnissii strain KCCM41679 was purchased from Korean Culture Center of Microorganisms (KCCM; Seoul, Republic of Korea) and cultivated in Luria-Bertani (LB) medium containing 3% NaCl (w/v) at 37°C with by shaking at 150-250 rpm on a rotary platform. *Escherichia coli* DH5α cells were from Life Technologies (Carlsbad, CA, USA) and also grown in LB medium at 37°C as described previously (Chang *et al*., 2005; Chang *et al*., 2007). This *E. coli* strain was routinely used as host cell for amplifying recombinant plasmid and expressing recombinant enzyme. Diisopropyl fluorophosphate (DFP), azocasein, ammonium sulphate, bovine serum albumin (BSA), trizma base, human fibrinogen, plasmin, plasminogen, collagen type IV, γ-globulin, and other chemicals were purchased from Sigma (St. Louis, MO, USA). Human FXIIIa and prothrombin were purchased from Enzyme Research Laboratories (South Bend, IN, USA). The chromatographic columns, including HiTrap Q FF, Source 15 Q 4.6/100 PE, Superdex 75 10/300 GL, and PD-10 were purchased from Amersham Pharmacia Biotech Co. (Uppsala, Sweden). YM10 membrane was obtained from Millipore (Billerica, MA, USA). Yeast extract, tryptone, and Bacto agar were obtained from Becton Dickinson (Baltimore, MD, USA). The restriction enzyme *Eco*RI and the T4 DNA ligase were purchased from New England BioLabs (Beverly, MA, USA). PCR purification kit and *i-Pfu* DNA polymerase were from iNtRON Biotechnology (Seongnam, Korea). Plasmid extraction kit, 100 bp DNA ladder, and *λ/Hin*dIII marker were purchased from BiONEER (Daejeon, Korea). Anyfusion was from Genemed Inc. (Seoul, Korea). Plasmid pFLAG-ATS was purchased from Sigma (St. Louis, MO, USA). Human plasma was prepared

as described previously (Adkins *et al*., 2002; Anderson *et al*., 1977) under an Institutional Review Board (IRB No. Chosun 2016-10-005-009) issued by Chosun University Hospital (Gwangju, Korea).

2-2. Experimental animals

Sprague–Dawley (SD) rats and BALB/c mice were purchased from OrientBio (Seongnam, Korea) and all animal procedures were conducted in compliance with protocols approved by the Chosun University Institutional Animal Care and Use Committee (IACUC) (Gwangju, Korea) under approval numbers CIACUC2017-S0035 for rat and CIACUC2019-A0016 for the mouse. During the animal acclimation, the animals were housed in stainless steel cages with noncontact bedding and maintained under controlled environmental conditions (22 ± 2°C, 12 h light/dark cycle), during which food (Certified Rodent Diet 5002; OrientBio) and tap water were given ad libitum.

2-3. Molecular cloning and nucleotide sequence analysis of *rvFMP* gene

The entire coding region of rvFMP gene was amplified by polymerase chain reaction (PCR) from the genomic DNA of *V. furnissii* KCCM41679 using *i-Pfu* DNA polymerase and a pair of forward (5′ -CAAGCTTCTCGAGAATTCATGAAAACATTACAAC-3′) and reverse (5′ -TGCAGGTACCCGGGAATTCTTAGTCCAGACGCAG-3′) primers (underlined bases indicate *Eco*RI restriction sites). The amplified PCR product (approximately 1.8 kb) was completely digested with *Eco*RI, ligated with *Eco*RI-cleaved pFLAG-ATS vector using T_4 DNA ligase, and then transformed into *E. coli* DH5α cells as

described (Kostylev *et al*., 2015). A recombinant plasmid containing 1.8 kb insert DNA was isolated and designated to as pvFMP harbouring *rvFMP* gene. The cloned gene was sequenced by dideoxy chain termination method as described previously (Park *et al*., 2011).

2-4. Expression and purification of a recombinant enzyme

An *E. coli* colony harbouring a recombinant plasmid pvFMP was initially grown overnight in 50 ml of LB medium containing 100 μg/ml of ampicillin at 37°C. Twenty ml of the culture was then inoculated into 2 L of LB broth containing 100 μg/ml of ampicillin and the cells were grown at 37°C until OD_{600} reached 0.8. Target protein expression was induced by adding 0.2 mM isopropyl-1-thio-β-d-galactopyranoside (IPTG), followed by overnight incubation at 37°C. The cells were then harvested by centrifugation, resuspended in 100 ml of lysis buffer [30 mM Tris-HCl, pH 8.0, 20% sucrose, 1 mM phenylmethylsulfonyl fluoride (PMSF), and 0.3 mg/ml lysozyme] to give an osmotic shock (Zhu *et al*., 1999), and incubated for 30 min at 4°C. The cell suspension was centrifuged for 20 min at 22,000 *xg* and 4°C and the supernatant containing periplasmic proteins was collected as described previously (Zhu *et al*., 1999). To purify rvFMP enzyme, the supernatant obtained was first subjected to an ammonium sulphate precipitation at a saturation concentration of 70% and the resulting protein pellet was collected by centrifuging for 40 min at 22,000 *xg* and 4°C. The proteins were then dissolved in 25 mM Tris-HCl buffer (pH 7.5) and applied to a PD-10 column to remove residual ammonium sulphate. The desalted proteins were loaded onto a HiTrap Q FF column equilibrated with 25 mM Tris-HCl (pH 7.5) and the bound proteins were eluted with a linear gradient of NaCl ranging from 0 to 0.7 M in the same buffer. The

active fractions were pooled, concentrated with an YM10 membrane, and desalted on a PD-10 column equilibrated with 25 mM Tris-HCl (pH 7.5). The desalted proteins were then loaded onto a Source Q 4.6/100 PE column equilibrated with 25 mM Tris-HCl (pH 7.5) and the bound proteins were eluted with a NaCl linear gradient of 0 to 0.4 M in the same buffer. The active fractions were pooled, concentrated, and finally loaded on a Superdex 75 10/300 GL gel filtration column equilibrated with 25 mM Tris-HCl (pH 7.5) containing 0.15 M NaCl. The active fractions were collected, pooled, and stored at -70°C as purified enzyme. In each purification step, protein concentration was determined by Bradford method as described (Bradford *et al*., 1976).

2-5. Protease activity assay and biochemical assessment

Azocasein assay was routinely used to measure protease activity through the chromatographic steps and also to examine the temperature and pH requirements for the purified enzyme as described previously (Chang *et al*., 2005). In typical azocasein assay, a reaction mixture (typically 200 μl) composed of enzyme to be tested, 25 mM Tris-HCl (pH 7.5), and 0.25% azocasein was incubated for 15 min at 37°C and then the reaction was terminated by adding 100 μl of 10% trichloroacetic acid. After centrifuging for 10 min at 13,000 *xg*, 200 μl of the supernatant was withdrawn and the absorbance at 440 nm was measured. In this assay, one unit of enzyme activity was defined as the amount of protease needed to digest 1 μg of azocasein per min. The buffer systems used for the assay were as follows: 25 mM sodium acetate (pH 4.0-6.0), 25 mM Tris-HCl (pH 6.5-9.5), and 25 mM glycine-NaOH (pH 10.0-11.0). Effects of various temperatures on enzyme activity were also examined using azocasein assay. To examine the thermo-stability of rvFMP, the enzyme (2 μg) was

pre-incubated at 37, 45, 55, 65, and 75°C for 20 min and reacted with 0.25% azocasein as a substrate for 15 min at 37°C. Apoenzyme of rvFMP (named apo-rvFMP) was prepared as described by Hirose *et al*. with minor modification. The purified rvFMP (100 μg) was dialyzed successively in 1,200 sample volumes each of 25 mM Tris-HCl (pH 7.5) containing 1 mM 1,10-PT, distilled water, and then 25 mM Tris-HCl (pH 7.5) for each 24 h at 4°C. The enzyme activity of apo-rvFMP (1 μg) was also examined in the absence or presence of various concentrations of $ZnCl_2$ (0, 0.01, 0.02, 0.05, and 0.1 mM) with azocasein assay as described above.

2-6. N-terminal sequencing of the purified enzyme

Protein samples were separated by SDS-PAGE on a 10% gel and transferred to PVDF membrane in 10 mM 3-(cyclohexylamino)-1-propanesulfonic acid (CAPS) buffer (pH 11.0) containing 10% methanol. Target bands were excised from the blot and subjected to N-terminal sequencing as described previously (Chang *et al*., 2005). The sequencing was performed using Edman degradation in Korea Basic Research Institute (Seoul, Korea) with a Procise 491 HT protein Sequencer (Applied Biosystems).

2-7. rvFMP-mediated cleavage of FXII, FXI, FX, and PPK

The reaction mixture consisted of 10 μg each of proteins to be digested (FXII, FXI, FX, and PPK) and 0.2 μg of rvFMP in a reaction buffer (25 mM Tris –HCl, pH 7.5, 0.9% NaCl, and 0.1 mg/ml BSA) was incubated for 1 or 5 min at 37°C. Thereafter, the reaction was terminated by the addition of 1 mM of 1,10-PT and the resulting products were electrophoresed on 12% SDS–

polyacrylamide gel, followed by staining with Coomassie brilliant blue to visualize (Park *et al*., 2014).

2-8. Activation of FXII, FXI, FX, and PPK by rvFMP

The reaction mixture consisted of 5 μg each of zymogens (FXII, FXI, FX, and PPK) and 0.2 μg of rvFMP in the same reaction buffer (25 mM Tris–HCl, pH 7.5, 0.1 mg/ml BSA, and 0.9% NaCl) was incubated for 1 or 5 min at 37°C and the reaction was terminated by the addition of 1 mM of 1,10-PT. Thereafter, the activated enzyme activities were observed as follows: FXIIa, FXIa and FXa activities were examined with the chromogenic substrate S-2302, S-2366, and S-2765 in which the increases in absorbance at 405 nm were monitored every 30 s for 10 min at 37°C in a 96-well plate reader (Molecular Devices). Kallikrein activity was assayed with 0.4 mM of H-D-Val-Leu-Arg-AFC by measuring λ_{em}= 505 nm and λ_{ex}= 400 nm every 30 s at 37°C for 10 min in a micro spectrofluorometer (Molecular Devices), from which the activity resulted was expressed as the relative fluorescence unit (RFU) (Park *et al*., 2014).

2-9. Activation of the components of the contact system in plasma milieu by rvFMP

Human plasma was prepared as follows: blood samples collected from healthy volunteers were put into a BD vacutainer tube containing 0.072 ml of 7.5% EDTA (Becton and Dickinson, NJ, USA) to prevent coagulation and centrifuged for 15 min at 3000 *xg* to remove blood cells (Park JW *et al*., 2013). The resulting plasma was stored at -70°C until used and diluted with phosphate-buffered saline (PBS) to a final concentration of 10%. To examine the

activation of contact system components, 90 μl of 10% plasma and 10 μl of rvFMP (1 μg) were mixed in the presence or absence of 1 mM of 1,10-PT and then 0.4 mM each of various synthetic peptide substrates (S-2302 for FXIIa, S-2366 for FXIa, S-2765 for FXa and H-D-Val-Leu-Arg-AFC for kallikrein) was added. The activity produced was then monitored every 2 min for 30 min at 37°C as described in Section 2-8.

2-10. Fibrin(ogen)olytic activity assay

Fibrinogenolytic activity assay was performed in a reaction mixture (total 180 μl) consisted in 270 μg of fibrinogen and 4.5 μg of rvFMP enzyme in 25 mM Tris-HCl (pH 7.5) at 37°C. During the reaction, 20 μl each of sample was withdrawn at various time intervals and the reaction was stopped by adding 2 μl of 10 mM 1,10-PT and the resulting products were analysed by SDS-PAGE on a 12% gel as described previously (Chang *et al*., 2005; Chang *et al*., 2007). Fibrinolytic activity of the enzyme was measured on a fibrin plate (Chang *et al*., 2005) and also by a turbidity assay (Park *et al*., 2013; Bello *et al*., 2006). For the fibrin plate assay, the plate was prepared by mixing 2 ml of 1% agarose, 2 ml of 1% fibrinogen, and 70 μl of 17.7 U/ml thrombin in 25 mM Tris-HCl (pH 7.5) and then allowed to harden at room temperature (RT) for 2 h. Thereafter, 20 μl each of Tris-buffered saline (TBS; pH 7.5) as a negative control, purified enzyme (2 μg) or plasmin (2 μg) as a positive control was inoculated into the wells (3 mm in diameter) that were pre-made in the plate and incubated for 5 h at 37°C to visualize halo zones (Chang *et al*., 2005). On the other hands, turbidity assay was performed by determining the decrease in turbidity of fibrin polymers in a 96-well plate as described previously (Park *et al*., 2013), in which 90 μl of 1 mg/ml fibrinogen (dissolved in 25 mM Tris-HCl, pH 7.5) were mixed

with 10 μl of 17.7 U/ml thrombin and then incubated for 1 h at 25°C to allow the formation of fibrin polymers. Thereafter, rvFMP (2, 4, or 6 μg) or plasmin (2 μg) was added and incubated for 2 h at 37°C, during which the decrease in absorbance at 350 nm was then recorded with a 96-well plate reader. The proteolytic ability of rvFMP to cross-linked fibrin (XL-fibrin) was investigated as follows: To prepare the XL-fibrin, 30 μg fibrinogen, 0.04 U thrombin, 0.004 U FXIIIa, 1 mM $CaCl_2$, and 25 mM Tris-HCl (pH 7.5) were mixed and incubated for 1 h at 25°C. The enzyme (0.5 μg) was then added to the XL-fibrin prepared and incubated at 37°C for 30 min. The reaction was stopped by adding 6 μl of 6 x SDS-PAGE sample buffer and heated for 3 min at 100°C. The resulting products were separated by SDS-PAGE on an 8% gel and visualized by staining with Coomassie Brilliant Blue as described previously (Park *et al*., 2013; Park *et al*., 2011).

2-11. Turbidimetric lysis assay of human plasma clot

Human plasma clot formation and lysis assay was performed as described previously (Carter Angela *et al*., 2007; Park *et al*., 2013). Briefly, 90 μl of 10% human blood plasma and 10 μl of 17.7 U thrombin were mixed and incubated for 1 h at RT to allow the formation of plasma clot. Thereafter, 10 μl each of TBS (pH 7.5), rvFMP (2, 4, and 6 μg), and plasmin (2 μg) was added and further incubated for 2 h at 37°C, during which the decrease in absorbance at 350 nm was recorded every 10 min with a 96-well plate reader. The relative turbidity was expressed as a percentage of a decrease in turbidity, relative to that at the beginning of incubation.

2-12. Measurement of thrombin time

Thrombin time (TT) was measured as described (Avecilla *et al*., 2012; Jacquemin *et al*., 2017). Typically, 10 μl each of rvFMP (1, 2, and 4 μg), heparin (0.001 or 0.01 μg), and uPA (5, 10, 20, and 40 μg) was mixed with 100 μl of human plasma and pre-incubated for 1 min at 37°C. To start the reaction, 10 μl of 17.7 U/ml thrombin and 50 μl of 20 mM $CaCl_2$ were added to the mixture and the time taken for clotting was measured using a KC-1 delta coagulometer (Amelung, Lemgo, Germany) at the end point, in which TT was calculated as the mean ± S.D. of triplicates.

2-13. $FeCl_3$-induced rat thrombosis model

To examine the effects of rvFMP and uPA on $FeCl_3$-induced arterial thrombosis (Li *et al*., 2017; Boulaftali *et al*., 2010), SD rats (220-250 g) were first anaesthetized with 1.5% isoflurane in a mixture of nitrous oxide (70%) and oxygen (30%), administered intravenously with PBS, uPA (5.24 mg/kg), or rvFMP (10, 25, 50, 75, and 100 μg/kg), and kept for 10 min. Vessel segments were then harvested from the right carotid arteries and fully covered with filter papers (6 mm x 6 mm) saturated with 4% $FeCl_3$ for 10 min to induce the thrombi. The induced regions (approximately 20 mm in length) were then cut out from the vessels and fixed overnight with 4% paraformaldehyde at 4°C. The fixed tissues were washed twice with ice-cold PBS and immobilized with commercially available specimen matrices called Tissue-Tek O.C.T. (optimal cutting temperature compound; Sakura Finetek, Torrance, CA, USA). The cryostat cuttings were then performed to obtain 20 μm slices in thickness with a microtome HM 400R (Microm International GmbH, Walldorf, Germany) as described (Barthel *et al*., 1990; Kuenzi *et al*., 1995). After mounting on slide glass, samples were observed and photographed under a microscope.

2-14. Carrageenan-induced rat tail thrombosis model

The *in vivo* anti-thrombolytic activity of rvFMP was examined using κ-carrageenan-induced thrombosis rat model (Wang *et al*., 2005; Hagimori *et al*., 2009 ; Choi *et al*., 2014; Majumdar *et al*., 2016) with a slight modification. SD rat (male; 6 weeks old) was administrated intravenously at tail with 200 μl each of PBS (pH 7.4; as negative control), urokinase (uPA; 5.24 mg/kg as positive control) or rvFMP (25, 50, 75, and 100 μg/kg) and kept for 10 min at RT. The area 13 cm away from the tip of the tail was tied and then κ-carrageenan (4 mg/kg) was injected intravenously to induce thrombus formation. After keeping on ice for 10 min, the tail was untied. The resulting thrombus length was measured and photographed 24 h later. The percentage of *in vivo* thrombus dissolution was also calculated using an equation shown by Majumdar *et al*.

2-15. Measurement of the concentration of fibrinogen in mouse plasma

The concentration of plasma fibrinogen was measured using ELISA with monoclonal anti-fibrinogen antibody (Sakamoto *et al*., 2018). To establish standard curve, 100 μl each of various concentrations of fibrinogen (0, 0.1, 0.2, 0.8, 1, 2, and 3 μg/ml; serially diluted in PBS, pH 7.5) was added into the wells of a 96 well immuno plate (SPL Life Sciences, Pocheon, Korea), incubated overnight at 4°C, washed with PBS (pH 7.5) three times, and then blocked with a blocking buffer (5% BSA in PBS, pH 7.5) for 2 h at room temperature. After washing the plate three times with PBS (pH 7.5), 100 μl of monoclonal anti-fibrinogen-α antibody (Santa Cruz Biotechnology Inc., CA, USA) (diluted 1:1,000 in blocking buffer) per well were added and incubated for 2 h

at room temperature. After the incubation, the wells were washed with PBS (pH 7.5) four times and incubated with 100 μl of anti-mouse IgG coupled to horseradish peroxidase (HRP) (Bioss Antibodies Inc., MA, USA) (diluted 1:1,000 in blocking buffer) for 2 h at room temperature. After washing with PBS (pH 7.5) five times, 100 μl of tetramethylbenzidine (TMB) was added and incubated for 20 min at room temperature. The reaction was stopped by adding 50 μl of 0.9 N sulfuric acid and the absorbance at 450 nm was measured using a SpectraMax M3 microplate reader (Molecular Devices, CA, USA). A standard curve for fibrinogen concentration was generated from the absorbance data using a sigmoidal 4 parameter curve fitting. To measure the plasma fibrinogen concentration *in vivo*, BALB/c mice (n = 4 per group) were injected with uPA (5.24 mg/kg) or rvFMP (0, 0.5, and 0.9 mg/kg) via intravenous tail vein and plasma samples were collected 10 min later. The plasma obtained was diluted 1:100 in PBS (pH 7.5) and 100 μl each of samples was used for ELISA, from which the concentration of fibrinogen was determined depending on the standard curve for fibrinogen. All ELISA experiments were performed in triplicate.

2-16. Measurement of the TNF-α production

Raw 264.7 cells (1 x 10^5) were plated on 48-well plates the day before rvFMP stimulation. Cells were treated with LPS or rvFMP (0-20 μg/ml) for 3 h at 37°C. The TNF-α protein levels were determined using ELISA kit (R&D system, Minneapolis, USA) according to the manufacturer's instruction. Absorbance at 450 nm was read with a 96-well microplate spectrophotometer (SpectraMax 190, Molecular Devices). Sample concentrations were determined by interpolation from a TNF-α standard curve.

2-17. Mouse tail bleeding assay

Bleeding time was measured using mouse tail bleeding assay as described previously (Liu *et al*., 2012). BALB/c mice (n = 4 per group) were anaesthetized with 1.5% isoflurane in a mixture of nitrous oxide (70%) and oxygen (30%), then injected with PBS, uPA (5.24 mg/kg) or rvFMP (0.5 and 0.9 mg/kg) into the tail veins, and kept for 10 min. The distal 5 mm segment of the tail was then amputated with a surgical scissor and submerged in 50 ml of PBS (pH 7.5) at 37°C. Bleeding time was then determined by measuring on/off bleeding cycles with a stop clock for up to 20 min.

2-18. Mouse lethality assay

Three 6-week-old BALB/c male mice for each group were injected tail intravenous with rvFMP of 0.5, 0.9, and 1.5 mg/kg, respectively. The injected mice were then monitored daily for 5 days to measure survival.

2-19. Degradation of artificial blood clots

The *in vitro* fibrinolytic effect of the antithrombotic agent was examined by an artificial blood clot degradation assay. An artificial blood clot was formed by spontaneous coagulation (5, 10, and 15 μg) in a glass test tube using fresh mouse blood. After 1 h, the artificial blood clot was rinsed, weighted, and then dipped in various concentrations of the rvFMP containing the antithrombotic agent at room temperature. Plasmin was used as a positive control condition. After 1 h, the residual thrombus was isolated and weighted. The dissolve ratio of thrombus was calculated using the following equation:

$$\text{The inhibition ratio} = \frac{\text{Weight}_a - \text{Weight}_b}{\text{Weight}_a} \times 100$$

where Weight_a was the thrombotic weight formed in a glass test tube and

$Weight_b$ was the residual thrombotic weight.

2-20. Cleavages of complements C3, C4, and C5 by rvFMP in plasma milieu

Human plasma was diluted with PBS (pH 7.5) to a final concentration of 10%. Reaction mixtures consisting of 10 μl of 10% human plasma and rvFMP (10, 20, 30, or 40 ng) diluted in PBS (pH 7.5) were incubated for 3 min at 37°C. Thereafter, the reactions were terminated by the addition of 1 mM of 1,10-PT as described previously. The cleaved products were separated by SDS-PAGE and detected by Western blottings with corresponding antibodies.

2-21. Sodium dodecyl sulfate-polyacrylamide gel electrophoresis (SDS-PAGE) and Western blot analysis

SDS-PAGE was performed according to the method of Laemmli (Laemmli *et al.,* 1970). Protein samples were mixed with 6 × SDS-PAGE sample buffer, heated at 3 min at 100°C and then protein samples and protein marker were loaded onto 10% or 15% polyacrylamide gel. After the electrophoresis, protein bands were visualized by staining the gel with Coomassie brilliant blue. The electrophoresed proteins were then transferred onto PVDF membrane (Bio-Rad, Hercules, CA, USA) and blocked with 5% skim milk in TBS-T (25 mM Tris-HCl, pH 8.0, 150 mM NaCl, and 0.1% Tween 20) at room temperature (RT) for 2 h. The membrane was then incubated with primary antibodies (1:4000 diluted in the blocking buffer) overnight at 4°C. After washing six times with TBS-T buffer, the membrane was then incubated with HRP-conjugated secondary antibodies (1:4000 diluted in the blocking buffer) at RT for 2 h and washed five times with

TBS-T buffer. The signals were detected using EZ-Western Lumi Plus system (DaeilLab Service, Seoul, Korea).

2-22. Statistical analysis

All statistical data and graphs were analyzed using SigmaPlot 10.0 (Systat Software Inc., La Jolla, CA). Data were expressed as mean ± standard error of mean (S.E.M) and statistical significance was determined by *t*-test using SigmaPlot software. $p < 0.05$ was considered a statistical significance.

3. RESULTS AND DISCUSSION

3-1. Purification and characterization of rvFMP

3-1-1. Molecular cloning and purification of a recombinant protease rvFMP expressed in *E. coli*

Vibrio furnissii KCCM41679 produces an extracellular protease named vFMP (data not shown). The full-length coding region of the *vFMP* gene was amplified by using polymerase chain reaction (PCR) from the chromosomal DNA of *V. furnissii* KCCM41679 as described in Materials and methods. A PCR product (1.8 kb) obtained was cleaved with *Eco*RI and then ligated to *Eco*RI-cut pFLAG-ATS vector (data not shown). The resulting recombinant plasmid constructed (approximately 7.2 kb in total size) was designated as pvFMP and the insert DNA was sequenced (Fig. 5). The sequence data of the cloned gene have been submitted to the GenBank database under an accession number MG954380. The sequencing results showed that the insert DNA contains an open reading frame composed of 1,827 nucleotides, which could encode 608 amino acids with a predicted molecular mass of 67443.71 Da (Fig. 6). The start and stop codons of cloned gene were found to be ATG and TAA, respectively. When the deduced amino acid sequence of cloned gene was compared with those of five other Vibrio-derived proteases from *V. fluvialis* (WP_020431607.1), *Vibrio* sp. RC586 (EEY99547.1), *V. anguillarum* (AAM15681.1), *V. mimicus* (BAG30958.1), and *V. vulnificus* (ALM73800.1) (number in parenthesis indicates GenBank accession number), there was an average of approximately 55.8% sequence similarity (Fig. 6). In addition, the sequence identity between their mature peptide regions was much higher to be an average of 80.8%, suggesting

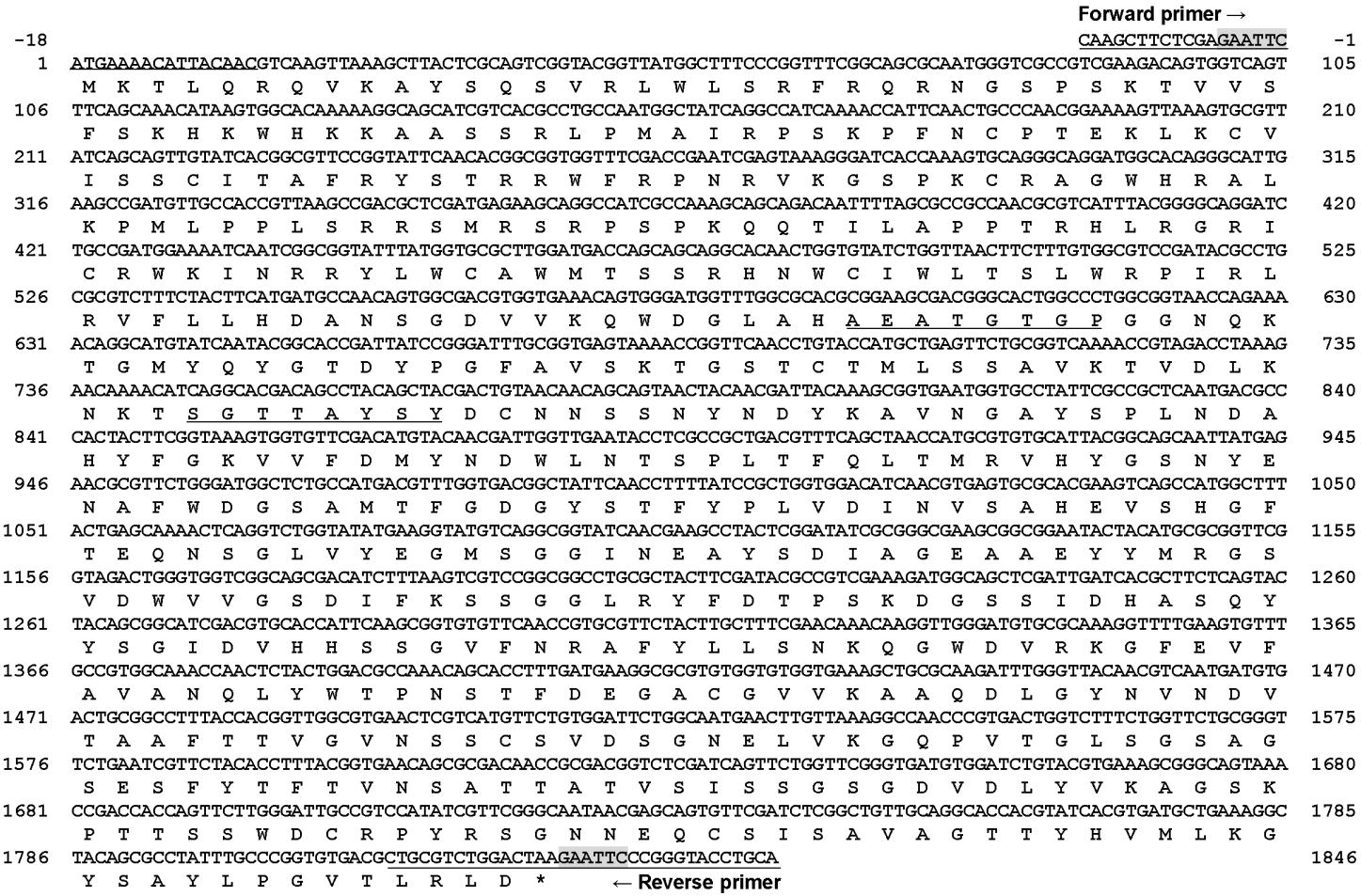

Fig. 5. The nucleotide and the deduced amino acid sequences of the cloned vFMP-encoding gene. The cloned gene contains an open reading frame composed of 1,827 nucleotides, which can encode 608 amino acids with a predicted molecular mass of 67,443.71 Da.

Fig. 6. Alignment of the amino acid sequence of rvFMP-44 with those of vibrio-derived metalloproteases.

(To be continued)

Putative signal peptide (24 amino acids), propeptide (173 amino acids), and mature protease (411 amino acids) regions that are located in prepro-rvFMP (total 608 amino acids) are compared with those of five vibrio proteases. The N-terminal start points of rvFMP-44 (411 amino acids) and rvFMP-39 (360 amino acids) are indicated by right-angled arrows and the authentic amino acid sequences found from the N-termini of rvFMP-44 and rvFMP-39 by N-terminal sequencings are also underlined. A putative zinc-binding HEXXHG-X_{18}-E motif containing $H^{344}EXXH^{348}$ and E^{368} is shown by gray-coloured boxes. The alignment was performed with the software Clustal W2 and the sequence similarities are expressed as identical (*), strongly similar (:), and weakly similar (.).

that they are highly conserved proteases. Data from the sequence comparison also showed that the cloned gene could produce a prepro-rvFMP composed of 608 amino acids as described above, which is organized with a signal peptide (24 amino acids), an N-terminal propeptide (173 amino acids), and a mature peptide (411 amino acids) containing a typical Zn^{2+}-binding motif (HEXXHG-X_{18}-E) (Hooper *et al*., 1994) (Fig. 6) that is often found from other bacterial metalloproteases. These results suggest rvFMP can be a zinc-metalloprotease, although the actual role(s) of this putative zinc-binding motif still remains to be elucidated further by using site-directed mutagenesis. To express the cloned *vFMP* gene, the plasmid pvFMP was transformed into *E. coli* DH5α cells and the recombinant enzyme (named rvFMP) was induced with IPTG. The recombinant enzyme expressed was purified from the periplasmic proteins of the cells using an ammonium sulphate precipitation and three chromatographic steps employing HiTrap Q, Source Q, and Superdex G-75 columns in order (data not shown). The purified enzyme appeared to be homogeneous and its apparent molecular mass was approximately 44 kDa (named rvFMP-44) or 39 kDa (called rvFMP-39) as judged by SDS-PAGE (Fig. 7). The purification steps are summarized in Table 3. The specific activity of finally purified enzyme was estimated to be 1,025.6 U/mg proteins as judged by azocasein assay and 0.9 mg of enzyme could be obtained from 3,539 mg of initial periplasmic lysate (Table 3). The preliminary N-terminal sequencing results showed that the N-termini of rvFMP-44 and rvFMP-39 were composed of AEATGTGP and SGTTAYSY, respectively (Fig. 8), which could be found from the deduced amino acid sequence of the cloned gene (Fig. 6). Based on these results, it was postulated that the protease is initially produced as a form of zymogen (named prepro-rvFMP), converted to an active rvFMP-44 by losing the N-terminal 197 amino acids that compose the signal peptide (24 amino acids)

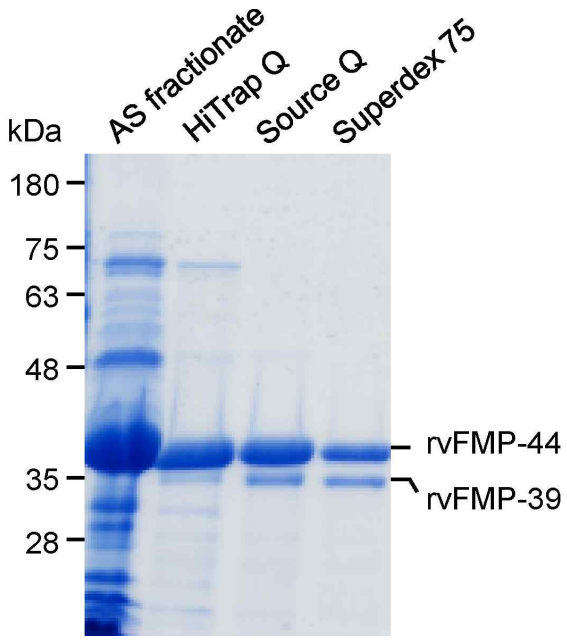

Fig. 7. Analysis of the purified proteins obtained by each chromatographic step as indicated on 12% SDS-polyacrylamide gel. Proteins collected from each purification step were electrophoresed on a 12% SDS-polyacrylamide gel and stained with Coomassie brilliant blue to visualize.

Table 3. Summary of the purification of rvFMP from *E. coli* harbouring pvFMP.

Purification step	Total protein (mg)	Total activity (U)[a]	Specific activity (U/mg)	Yield (%)[b]
Crude cell extract	3,539	706,060.5	199.5	100
0-70% (NH4)2SO4	39.7	9,513.7	242.4	1.12
HiTrap Q	9.3	5,005.3	538.2	0.26
Source Q	2.5	1,303.7	651.9	0.07
Superdex 75	0.9	923.0	1,025.6	0.025

[a]One unit of enzyme is defined as the amount of protease that catalyses the proteolysis of 1 μg of azocasein per min.
[b]Total activity in crude periplasmic extract is assigned the value of 100%. Data from two independent experiments are expressed as mean value ± S.D.

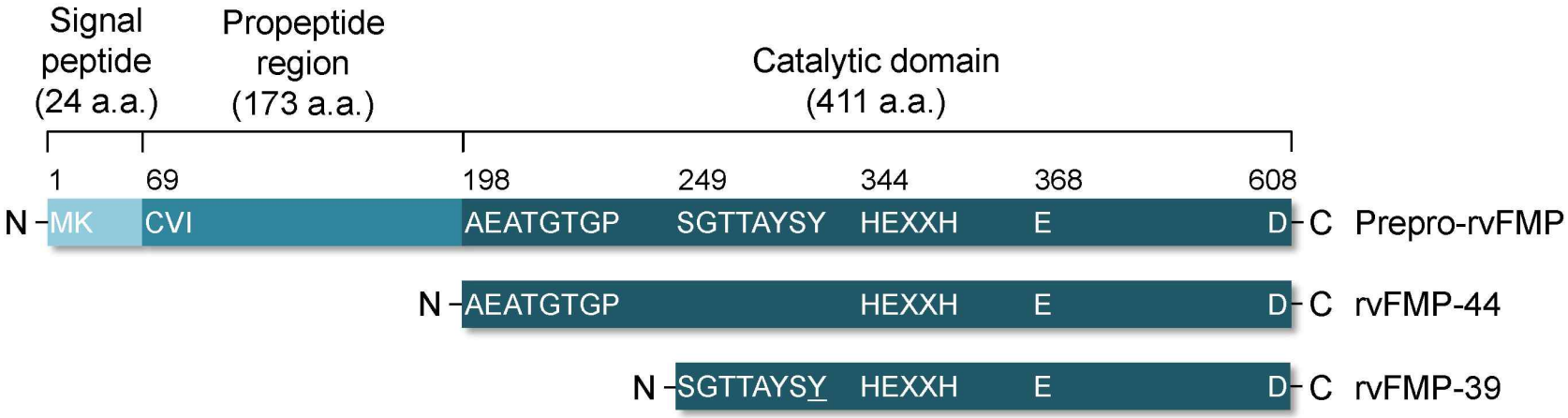

Fig. 8. Overall organization of rvFMP protease. Prepro-rvFMP protease is composed of 608 amino acids, in which three regions, composed of signal sequence (24 a.a.), propeptide (173 a.a.), and a catalytic domain (411 a.a.) are located. Signal peptide targets the protein for secretion. Propeptide may act as inhibitor for the proteolytic activity. Catalytic domain contains the catalytic machinery including a zinc-binding motif ($H^{344}EXXH^{348}$-E^{368}).

and the propeptide regions (173 amino acids) during the extracellular secretion, and in turn an N-terminal 51 amino acid stretch breaks off further to remain rvFMP-39, possibly resulted from the procedure of purification (Figs. 7 and 8). However, the actual roles of the signal peptide and propeptide regions of prepro-rvFMP should be elucidated further in terms of the secretion into periplasmic space and in controlling enzyme activity. There are reports that some bacterial metalloproteases also have a tendency to undergo the auto-degradation, resulting in remaining two forms of enzymes (mature and truncated enzymes) during the course of secretion and physical purification (Chang *et al*., 2007; Kothary *et al*., 2007; Miyoshi *et al*., 1997). As for an extracellular metalloproteinase called vEP-45 protease (45 kDa in size) from *V. vulnificus*, its N-terminal propeptide acts in fact as both an inhibitor of and a substrate for the enzyme (Chang *et al.,* 2005). It has also been reported that some bacterial metalloproteases undergo auto-cleavage, resulting in producing two forms of enzymes (mature and truncated enzymes) during the course of secretion and physical purification (Chang *et al*., 2007; Kothary *et al*., 2007; Miyoshi *et al*., 1997). For example, a Zn^{2+}-metalloproteinase vEP-45 has a proteolytic activity to be auto-degraded, producing another protease vEP-34 (34 kDa in size) by cleaving off the N-terminal amino acid stretch.

3-1-2. Biochemical properties of rvFMP protease

The purified rvFMP enzyme exhibited an optimal proteolytic activity under pH 6.5-8.0 (Fig. 9) and at the temperature range of 30-50°C (Fig. 10). In addition, the relative protease activity of rvFMP was not significantly affected at 37, 45, and 55°C however, it decreased dramatically to 4.1 and 0.6% at 65 and 75°C, respectively, compared with that of at 37°C when the enzyme (2 μg)

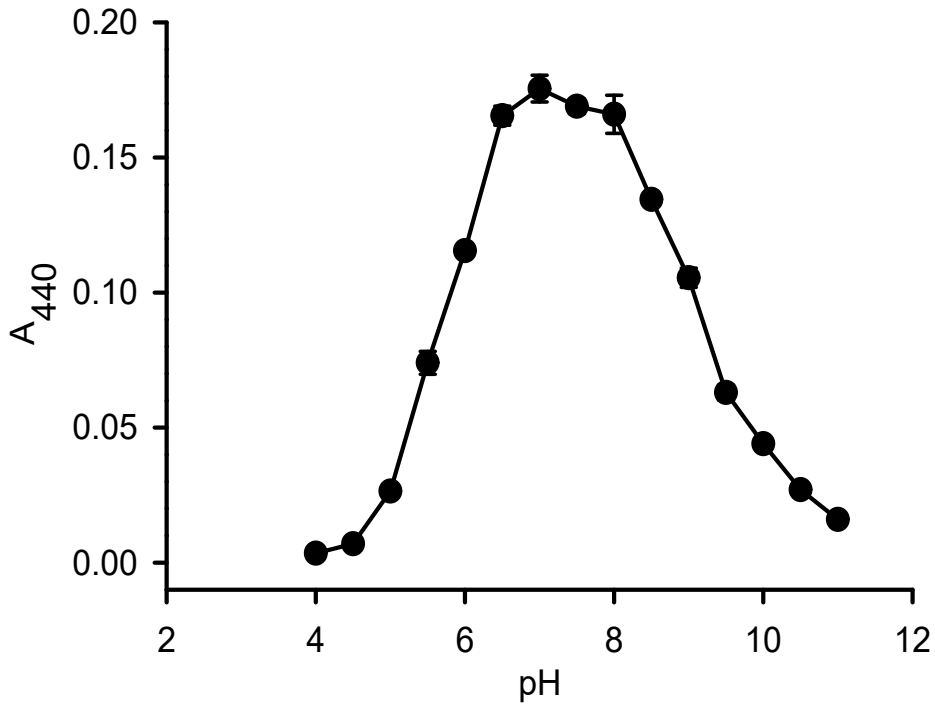

Fig. 9. Effects of various pHs on the enzyme activity of rvFMP enzyme. rvFMP enzyme (0.5 μg) was incubated at 37°C for 30 min with azocasein as a substrate under different pH conditions and the absorbance at 440 nm was measured.

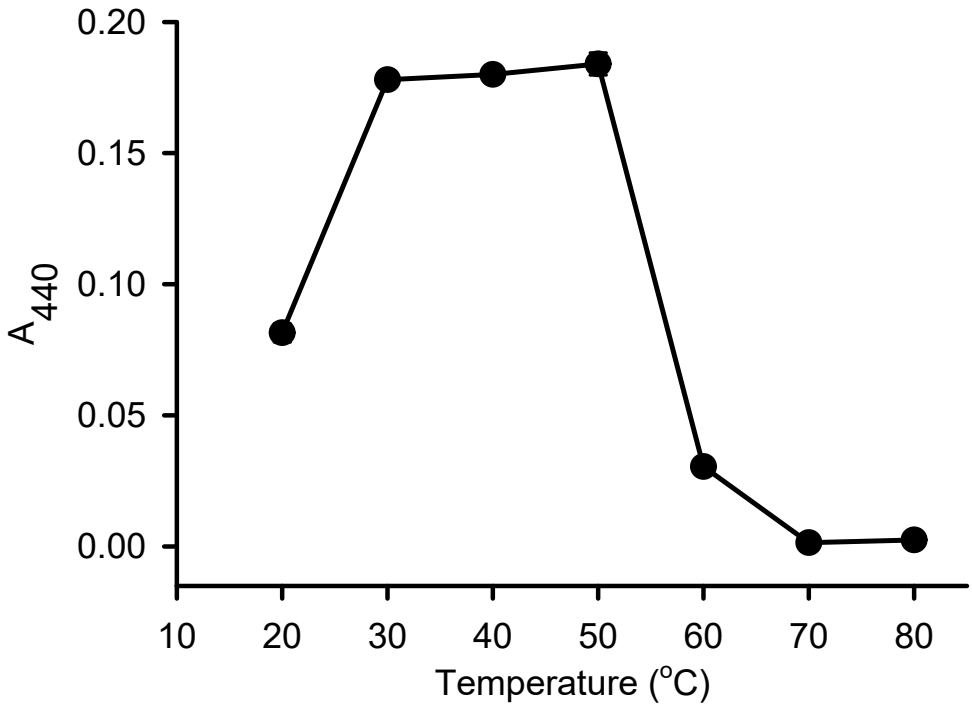

Fig. 10. Effect of temperature on the enzyme activity of rvFMP enzyme. rvFMP enzyme (0.5 μg) was incubated with azocasein as a substrate at various temperatures for 30 min as indicated, and the absorbance at 440 nm was measured.

was pre-incubated at 37, 45, 55, 65, and 75°C for 20 minutes and reacted with azocasein as a substrate at 37°C for 15 minutes under pH 7.5 (Fig. 11). The loss of enzyme activity seemed to be directly related to the degradation of rvFMP under the high incubation temperature. As shown in Fig. 12, rvFMP was degraded totally under higher temperature than 65°C, however, the event could be significantly prevented by the addition of 1,10-PT (1 mM) or $NiCl_2$ (1 mM) as judged by SDS-PAGE (Fig. 12). The rvFMP-39 seemed to be more sensitive to thermal degradation than rvFMP-44, as it started the degradation even at 55°C (Fig. 12). These results suggest that rvFMP can be destabilized and auto-cleaved under high temperature, as in vEP-45 protease (Chang *et al*., 2005). All these results suggest that rvFMP can be stable up to 45°C and auto-degraded at higher temperatures than 65°C. The proteolytic activity of rvFMP was completely inhibited by a typical metalloprotease inhibitor 1,10-PT, but not by a serine protease inhibitor DFP. Other protease inhibitors, including TPCK (inhibitors of chymotrypsin-like serine proteases), TLCK, PMSF (typical inhibitor of all serine proteases), and aprotinin (inhibitors of chymotrypsin-like serine proteases) showed no significant inhibitory effects on the enzyme activity, whereas divalent cation chelators such as EDTA and EGTA exhibited inhibitory (Table 4). These results suggest that the enzyme is a typical metalloprotease. Divalent cations such as Ca^{2+}, Mg^{2+}, and Mn^{2+} showed no effects on the enzyme activity, whereas Cu^{2+} and Ni^{2+} was inhibitory in significant at a final concentration of 1 mM (Table 4). Azocasein assays also showed that the proteolytic activity of apo-rvFMP enzyme decreased to approximately 20%, compared to that of its holoenzyme, whereas the activities restored to 106.4%, 108.2, 110.7, and 102.3% by the additions of 0.01, 0.02, 0.05, and 0.1 mM of $ZnCl_2$, respectively, compared that of apo-rvFMP only (Fig. 13). These results suggest that rvFMP is a zinc-metalloprotease. The rvFMP protease was able to

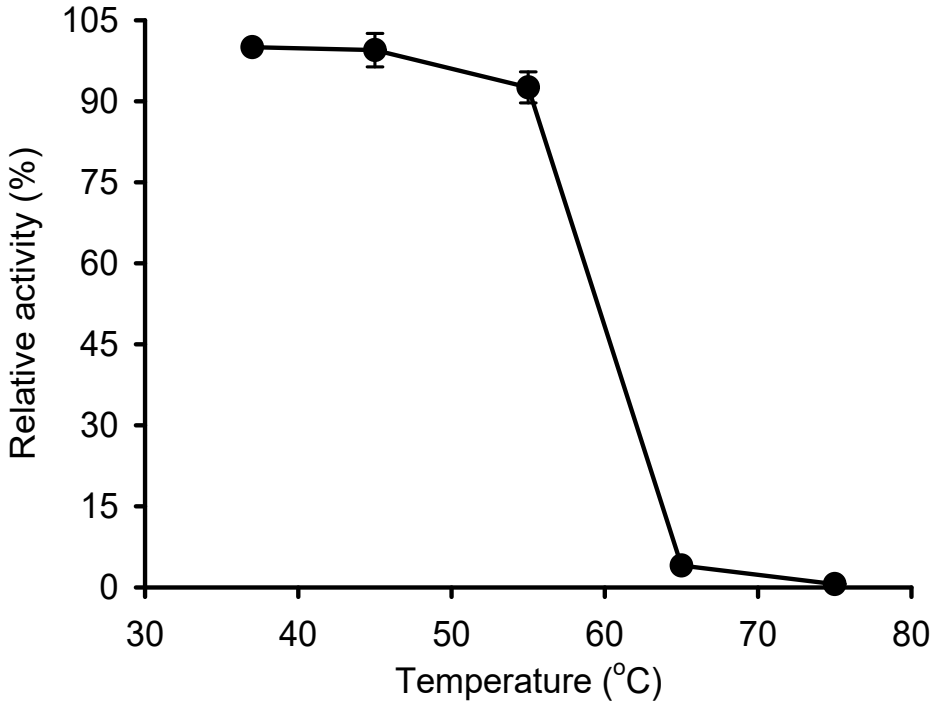

Fig. 11. The thermo-stability of rvFMP under various temperatures. rvFMP was pre-incubated at 37, 45, 55, 65, and 75°C for 20 min and reacted with azocasein as a substrate at 37°C for 15 min under pH 7.5.

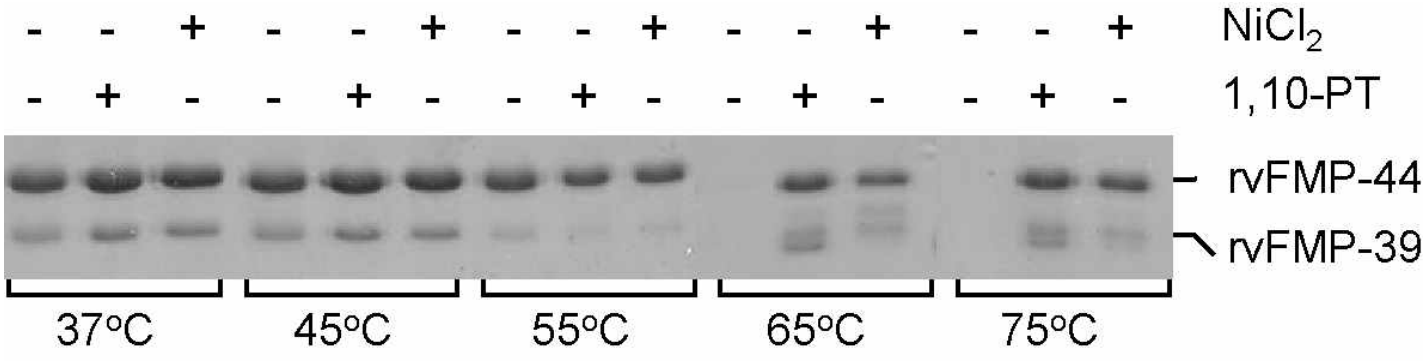

Fig. 12. Examination of the thermo-stability of rvFMP under various temperatures. rvFMP (2 μg) was incubated at 37, 45, 55, 65, or 75°C for 20 min in the absence (-) or presence (+) of $NiCl_2$ (1 mM) or 1,10-PT (1 mM), separated by SDS-PAGE on a 12% gel, and stained with Coomassie brilliant blue to visualize.

Table 4. Effects of various protease inhibitors and metal ions on rvFMP protease activity.

Additive	Concentration (mM)	Relative activity (%)[a]
Control	-	100 ± 0.1
TPCK	0.1	82 ± 0.07
TLCK	1	98 ± 0.0
PMSF	1	89 ± 0.01
Aprotinin	0.1	100 ± 0.00
EGTA	1	64 ± 0.02
EDTA	1	67 ± 0.01
DTT	1	56 ± 0.01
DFP	1	100 ± 0.02
1,10-PT	1	0 ± 0
Ca^{2+}	1	104 ± 0.02
Cu^{2+}	1	0 ± 0
Mg^{2+}	1	101 ± 0.0
Mn^{2+}	1	97 ± 0.01
Ni^{2+}	1	26 ± 0.01
Zn^{2+}	0.1	99 ± 0.75

[a]rvFMP protease activity was assayed with azocasein as a substrate with or without the corresponding additives at 37°C for 20 min.

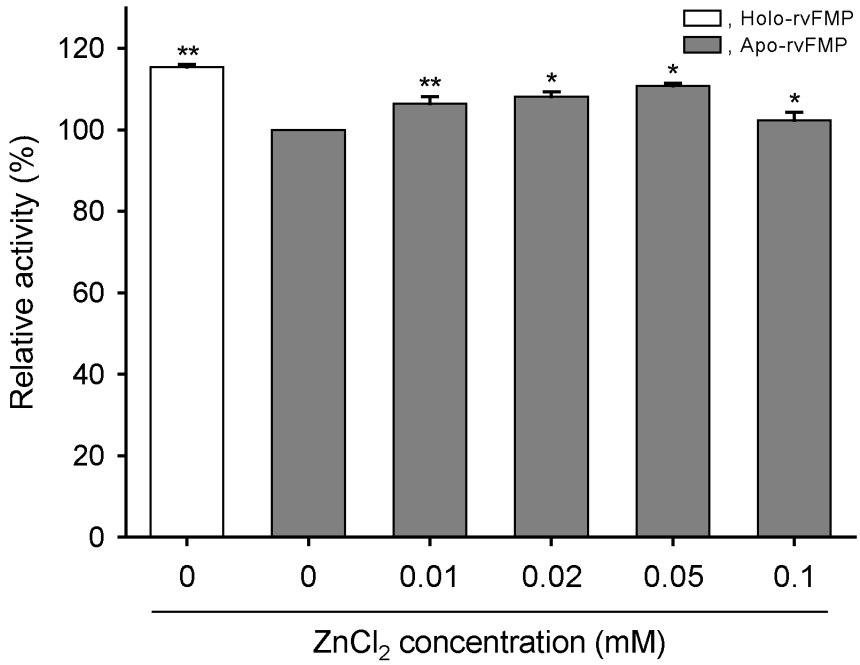

Fig. 13. Effects of various concentrations of $ZnCl_2$ on the proteolytic activities of holo- and apo-rvFMP enzymes. Apoenzyme of rvFMP (named apo-rvFMP) was prepared by dialyzing successively in 25 mM Tris-HCl (pH 7.5) containing 1 mM 1,10-PT, distilled water, and 25 mM Tris-HCl (pH 7.5) for each 24 h at 4°C and then azocasein assays were performed with 1 μg each of corresponding enzymes as described in Materials and methods. *, $p < 0.05$; **, $p < 0.005$ versus compared to that of holo-rvFMP.

cleave efficiently various plasma proteins, including BSA, fibrinogen, prothrombin, collagen type IV, and plasminogen, with a lowered cleavage of γ-globulin (Fig. 14). Among the protein substrates examined, prothrombin and fibrinogen were the most efficient substrates for the enzyme. The proteolytic cleavage site for rvFMP on protein substrate could be determined in part by N-terminal sequencings with two peptide fragments (P1 and P2 indicated in Fig. 14) from the fibrinogen digests. The sequences for P1 and P2 were found to be Val^{145}-Ile-Glu-Lys-Val-Gln-His-Ile^{152} located in α-chain and Val^{187}-Asn-Ser-Asn-Ile-Pro-Thr-Asn^{194} in β-chain, respectively. Based on these results, it is assumed that rvFMP can hydrolyse the peptide bond located in the amino side of Val^{145} or Val^{187} rather than the carboxyl side of Lys^{144} or Thr^{186} on fibrinogen substrate. Further studies are in progress to reveal the exact cleavage site of rvFMP.

3-1-3. Fibrin(ogen)olytic activity of rvFMP

The rvFMP enzyme showed the activity of fibrinogenolytic and fibrinolytic. The Aα and Bβ chains of fibrinogen could have been entirely cleaved by rvFMP within 1 minute with a mass ratio of 1:7.9 (enzyme *vs* fibrinogen). However, the γ-chain was more resistant to be digested (Fig. 15). The turbidity analysis showed that the relative turbidity of the fiber polymer decreases after being treated with plasmin (as a positive control) or rvFMP in a time-dependent manner (Fig. 16). These results suggest that rvFMP, like plasmin, has typical fibrous-source decomposition activity and can actively cleave fibrous polymers that are spontaneously polymerized from fibrous monomers (Ghosh *et al.,* 2012; Verstraete *et al.,* 2000).In addition to the digestion ability to fibrin polymers, rvFMP could also cleave the cross-linked fibrin (XL-fibrin) formed

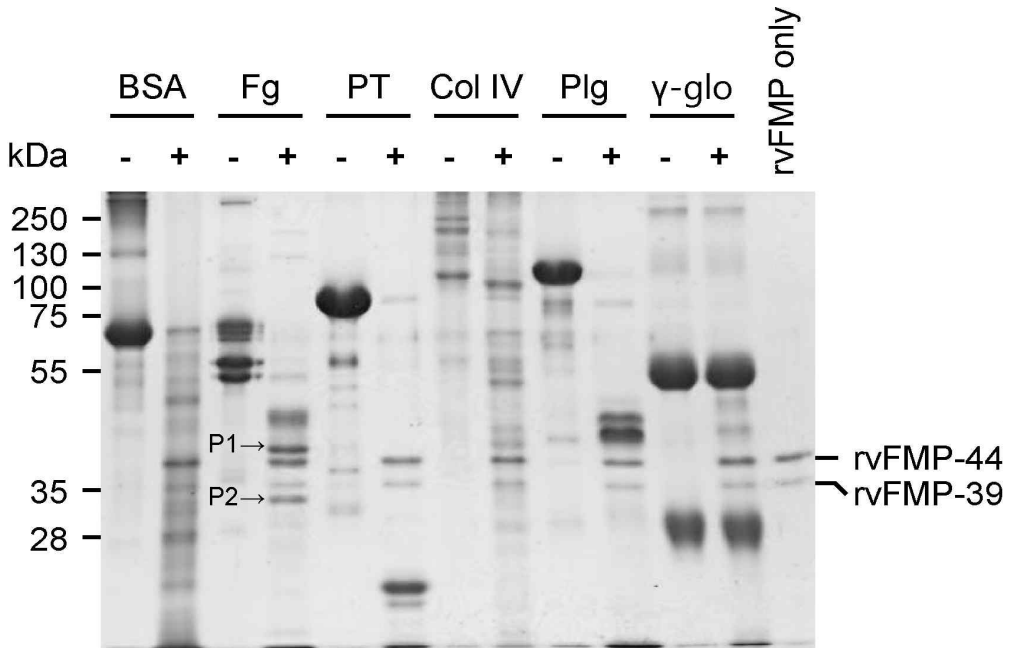

Fig. 14. Cleavage of various protein substrates by rvFMP. Various plasma proteins (each 10 μg) were reacted with rvFMP (0.5 μg) at room temperature for 20 minutes as indicated, separated by 12% SDS-PAGE, and stained with Coomassie brilliant blue to visualize. Symbols + and − represent the addition and the omission of rvFMP to the reactions, respectively. BSA, bovine serum albumin; Fg, fibrinogen; PT, prothrombin; Col IV, collagen type IV; Plg, plasminogen; γ-glo, γ-globulin. P1 and P2 indicate the peptide fragments, with which the determined the N-terminal sequences.

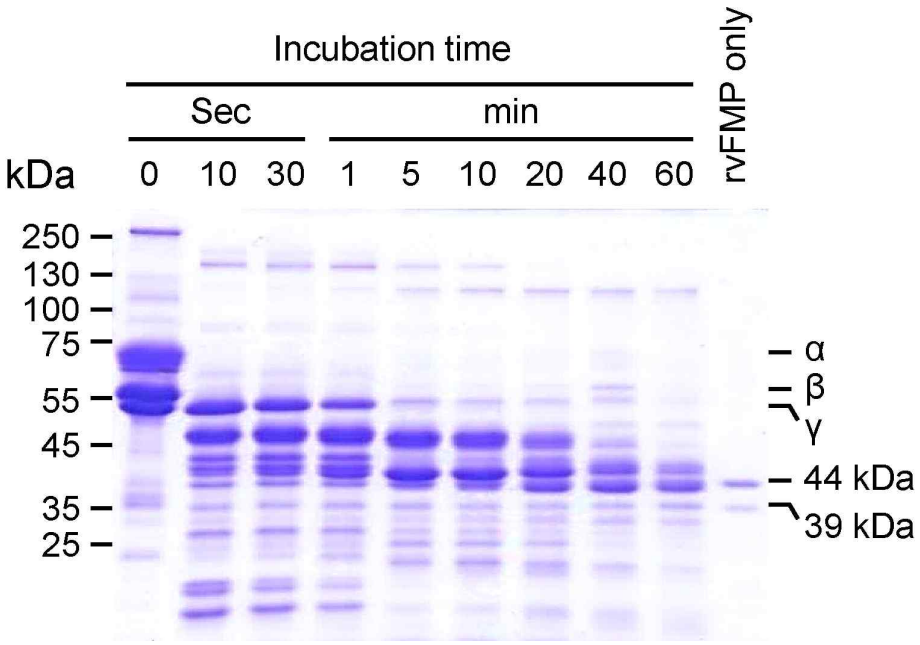

Fig. 15. SDS-PAGE analysis of fibrinogen cleavage by rvFMP. Fibrinogen (30 μg) was incubated with rvFMP (0.5 μg) for various time periods at 37°C as indicated. The resulting products were separated by SDS-PAGE on a 12% gel and stained with Coomassie brilliant blue to visualize.

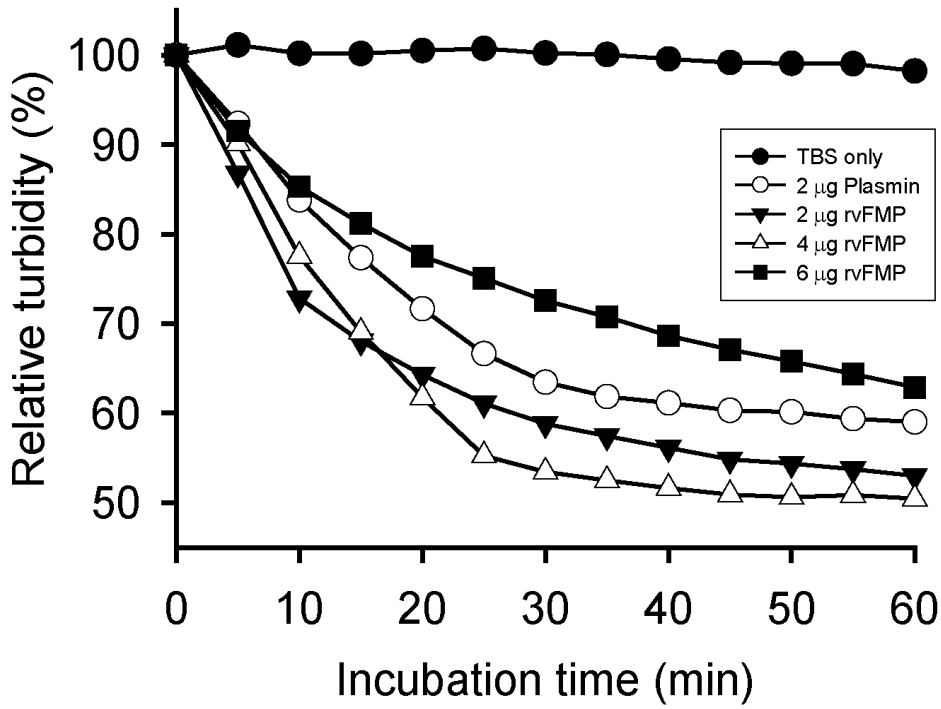

Fig. 16. Turbidity assay *in vitro*. To examine the proteolytic ability of rvFMP to fibrin polymers, 90 μl each of fibrinogen (1 mg/ml) was pre-treated with 10 μl of thrombin (17.7 U/ml) for 1 h at 37°C and then 10 μl of TBS (pH 7.5), plasmin (2 μg), or rvFMP (2, 4, and 6 μg) were added. The reaction was continued for 1 h at 37°C and the decrease in absorbance at 350 nm was recorded every 5 min using a 96-well plate reader. Relative turbidity is expressed as a percentage of a decrease in turbidity, relative to that at the beginning of incubation. Data are expressed as mean ± S.D. of triplicates.

under the presence of FXIIIa, as analyzed by SDS-PAGE (Fig. 17) and fibrin plate analysis (Fig. 18). The α-α chains of fibrin were susceptible to cleavage by the enzymes, with vulnerable to the γ-γ chains (Fig. 18). The ability of rvFMP to XL-fibrin cleavage was also examined on the fibrin plate. As shown in Fig. 18, clear halo zones appeared on the fibrin plate by inoculating plasmin (2 μg) and rvFMP (2 μg) with diameters of 0.7 cm and 1.1cm, respectively. These results indicate that rvFMP has apparent fibrin cleavage activity about 2.5 times stronger than the same amount of plasmin *in vitro*. Most fibrino(geno)lytic enzymes prefer to cleave the Aα and/or the Bβ chain(s) than the γ chain of fibrinogen (Swenson *et al.,* 2005; Assakura *et al*., 1994). In addition, some metalloproteases show somehow much stricter in digesting the fibrinogen chains. For example, α-fibrinogenases such as Leuc-A (Bello *et al*., 2006) and halysase (You *et al*., 2006) can digest α-chain only. In addition, β-fibrinogenases prefer B β-chain to Aα- and γ-chains in cleavingfibrinogen (Swenson *et al*., 2005). Plasmin and rvFMP, they can actively digest the Aα and Bβ chains of fibrinogen, with a limited proteolytic ability to cleave the γ-chain (Figs. 15 and 18).

3-1-4. Cleavage of fibrin clots by rvFMP and its effect on thrombin time in blood plasma milieu

It is well known that human blood plasma contains large amounts of proteins (approximately 60-85 mg/ml), including albumin, globulin, fibrinogen, (pro)enzymes and protease inhibitors (Anderson *et al.*, 1977) together with inorganic materials such as Na+, Cl^-, K^+, and Mg^{2+} (Adkins *et al.*, 2002). Therefore, it was necessary to examine how the protease activity of the rvFMP, mostly related with fibrin coagulation cleavage, could be affected by plasma

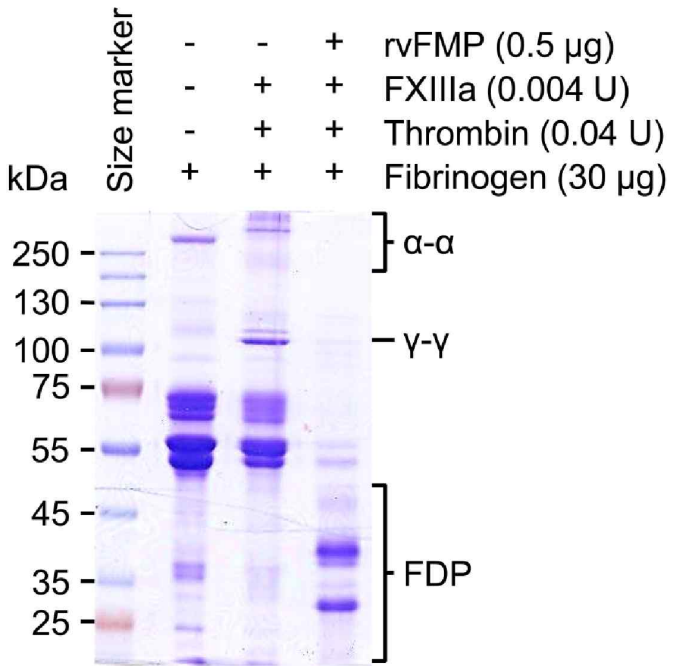

Fig. 17. SDS-PAGE analysis of cross-linked (XL)-fibrin cleavage by rvFMP. To allow the polymerization and cross-linking of fibrin monomers, fibrinogen (30 μg) and thrombin (0.04 U) were incubated in the presence of FXIIIa (0.004 U) for 1 h and the resulting XL-fibrin was then cleaved with rvFMP (0.5 μg) for 30 min at 37°C. The reaction products were separated by SDS-PAGE on an 8% gel and stained with Coomassie brilliant blue to visualize. Symbols '+' and '-' represent the addition and the omission of the corresponding additive, respectively. FDP means fibrin degradation products.

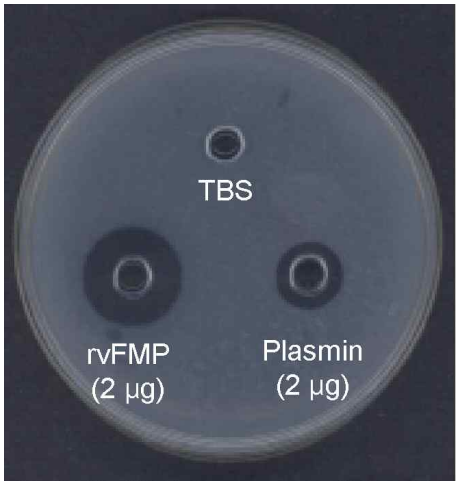

Fig. 18. Fibrin plate assay. To examine the fibrinolytic activity of rvFMP, TBS (pH 7.5), plasmin (2 μg), or rvFMP (2 μg) was inoculated into the wells pre-made in fibrin plate as indicated, incubated for 5 h at 37°C, and then photographed to show the halo zones appeared.

components such as serum albumin, intrinsic protease inhibitors and cation, as in multimodial CTSP protease from the polychaete *Cirriformia tentaculata* (Park *et al.,* 2005). As shown in Fig. 19, rvFMP can actively cleave fibrin coagulation formed in human plasma on a dose-dependent manner, as judged by turbidimetric lysis method (Carter *et al.,* 2007; Park *et al.,* 2005). The results obtained showed that 2, 4, and 6 μg of rvFMP decreased dose-dependently the turbidity of plasma clot to 8%, 18.3%, and 21.3%, respectively, at the incubation time points of 2 hours, compared to that of non-treated control (Fig. 19). Plasmin (2 μg) reduced turbidity to 9.3% under the same experimental conditions (Fig. 19). These results suggest that the rvFMP can digest fibrin coagulation in plasma environments, with almost the same activity as plasmin. The thrombin time [TT; also known as thrombin clotting time (TCT)] has been widely used for examining basically the conversion of fibrinogen to fibrin in platelet-poor plasma treated with thrombin (Avecilla *et al*., 2012), to which the time taken for the formation of a fibrin clot is measured (Jacquemin *et al*., 2017). In this study, the effect of rvFMP on TT in human plasma with added thrombin was investigated. As expected, 0.001 and 0.1 μg of heparin delayed TTs by 8 and 21 seconds, respectively, compared to PBS. The TTs were also delayed by 9.3, 20, and 34.6 sec when 10, 20, and 40 μg of uPA was added, respectively. As shown in Fig. 20, 1, 2, and 4 μg of rvFMP could delay the TTs to 8.6, 21, and 62.5 sec, respectively. These results clearly suggest that rvFMP has an ability to delay TT in plasma.

3-2. Effect of rvFMP on the thrombus formation in animal thrombosis models

3-2-1. Mouse lethality by rvFMP

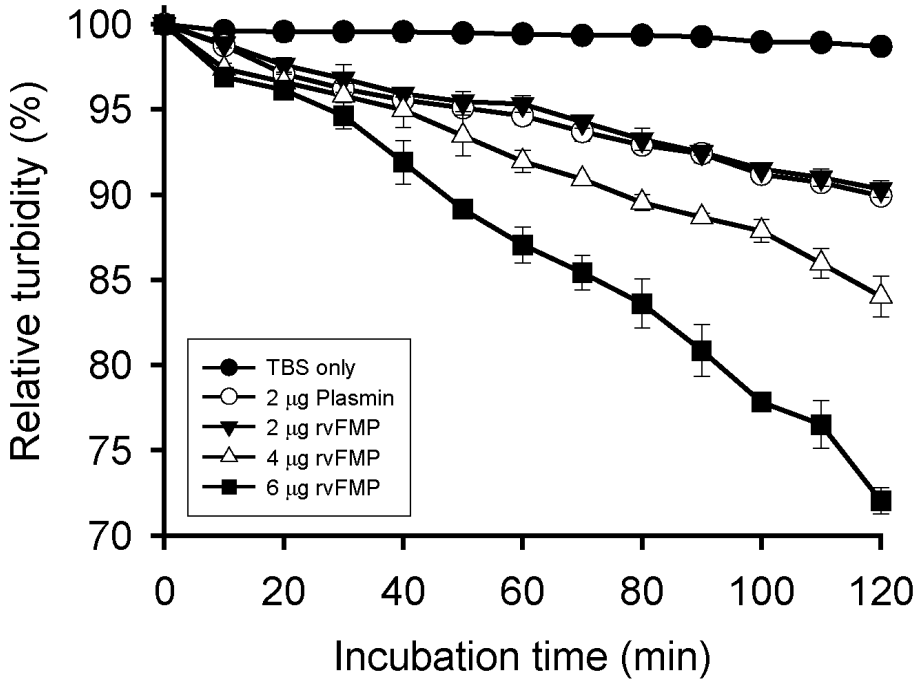

Fig. 19. Turbidity assay in plasma milieu. To examine the fibrinolytic activity of rvFMP in plasma, 90 μl of 10% human plasma was pre-treated with 10 μl of thrombin (17.7 U/ml) for 1 h at 37°C and then 10 μl of TBS (pH 7.5), plasmin (2 μg), or rvFMP (2, 4, and 6 μg) were added. The reaction was continued for 2 h at 37°C and the decrease in absorbance at 350 nm was recorded every 10 min using a 96-well plate reader. Relative turbidity is expressed as a percentage of a decrease in turbidity, relative to that at the beginning of incubation. Data are expressed as mean ± S.D. of triplicates.

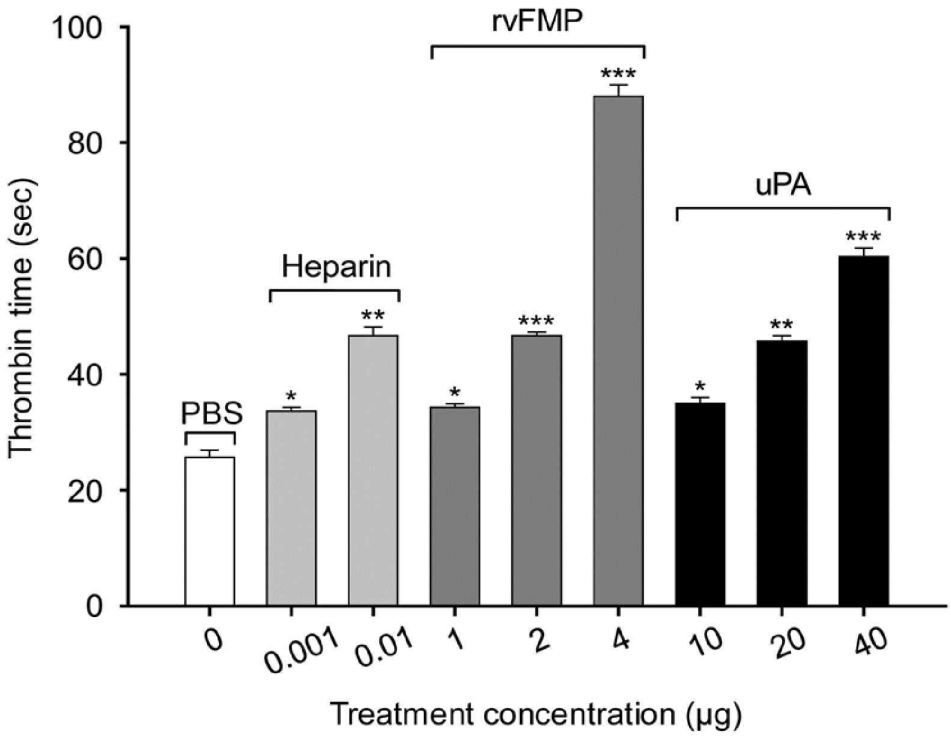

Fig. 20. Effect of rvFMP on thrombin time (TT) in human plasma. Ten μl each of PBS (pH 7.5), heparin (0.001 or 0.01 μg), rvFMP (1, 2, or 4 μg), and uPA (10, 20, or 40 μg) was mixed with 100 μl of human plasma and pre-incubated for 1 min at 37°C, followed by the additions of 10 μl of 17.7 U/ml of thrombin and 50 μl of 20 mM $CaCl_2$. TTs are expressed as mean S.D. of triplicates. *, $p < 0.001$; **, $p < 0.0001$; ***, $p < 0.00001$ versus compared to that of PBS-treated control group.

When various concentrations of rvFMP (0, 0.5, 0.9, and 1.5 mg/kg) were treated through mouse tail veins and monitored for 5 days, all groups of mice survived healthily with no internal bleedings (Fig. 21).

3-2-2. Effect of uPA or rvFMP on plasma fibrinogen concentration in mouse

In mice, uPA (5.24 mg/kg) could decrease the plasma fibrinogen concentration to about 5.9% compared to the non-treated control. Under the same experimental conditions, 0.5 and 0.9 mg/kg of rvFMP also reduced the fibrinogen concentrations to 4.8% and 6.9%, respectively (Fig. 22). These results suggest that rvFMP does not significantly induce the depletion of fibrinogen in plasma, compared to that by uPA (Hida *et al.,* 2004).

3-2-3. Effect of rvFMP on $FeCl_3$-induced thrombus formation in rat carotid artery

The effect of rvFMP on blood vessel thrombosis in rat carotid artery exposed to $FeCl_3$ was investigated (Fig. 23). As shown in Fig. 23, non-treated control (Fig. 23A), PBS (Fig. 23B), uPA (5.24 mg/kg) (Fig. 23C), or rvFMP (100 μg/kg) (Fig. 23D) did not form thrombi in the carotid artery and showed no effect, but vascular thrombi were caused by the exposure of $FeCl_3$ (Fig. 23E-L). As reported already, the development of vascular thrombi by $FeCl_3$ exposure decreased clearly by the pre-injection of uPA (5.24 mg/kg) (Fig. 23G) (Yu *et al.,* 2017). The pre-injections of various concentrations of rvFMP (10-100 μg/kg) also evidently reduced the formation of thrombi resulted from the exposure of $FeCl_3$ in the rat carotid artery (Fig. 23H-L). These results suggest

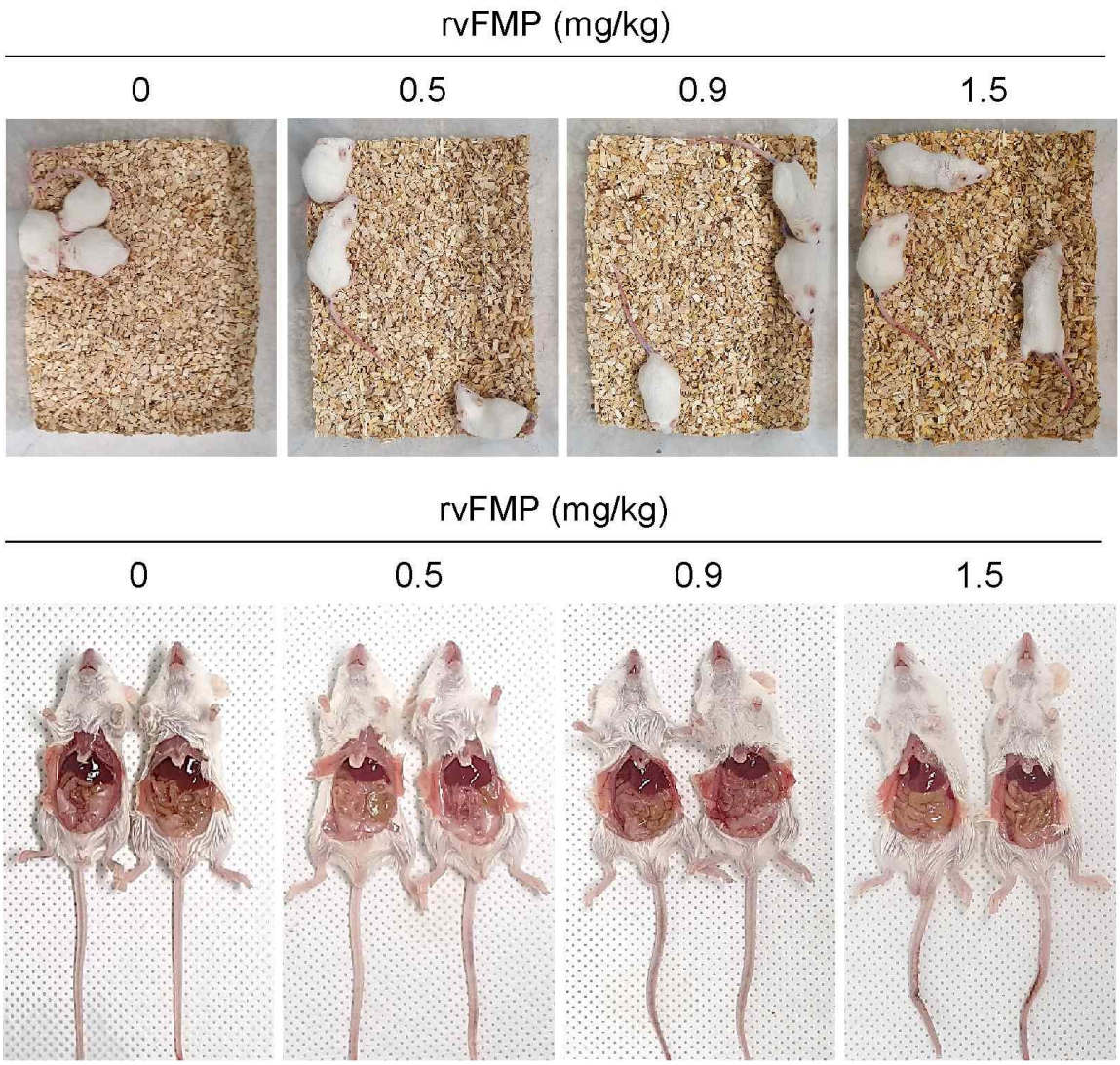

Fig. 21. Examination of lethal and internal bleeding effects of rvFMP on mice. Anatomical photograph showing no internal bleeding with rvFMP.

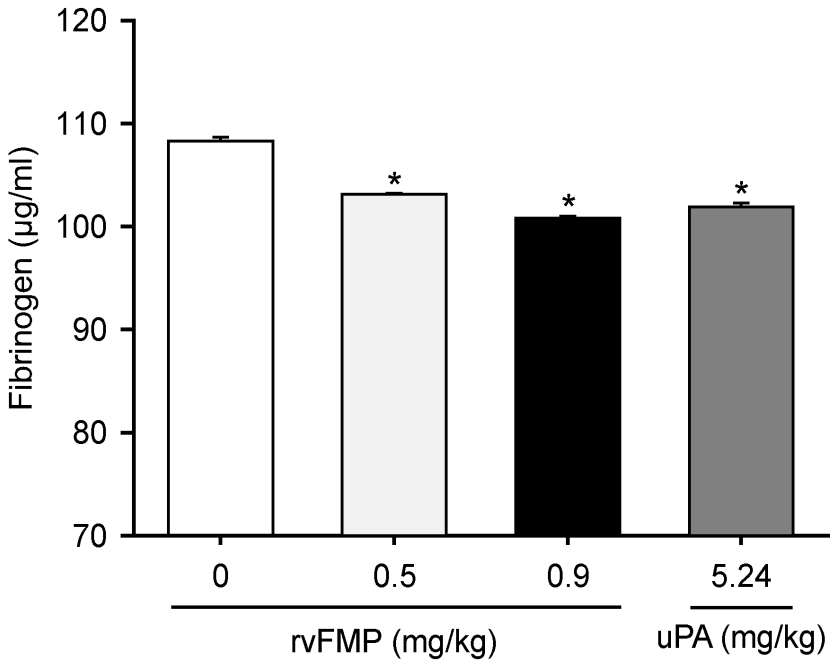

Fig. 22. Effect of uPA or rvFMP on plasma fibrinogen concentration in mouse. BALB/c mice (n = 4 per group) were administrated with various doses of rvFMP or uPA as indicated and plasma samples were collected 10 min later, from which the fibrinogen concentrations were measured using ELISA with monoclonal anti-fibrinogen antibody as described in Materials and methods. $p < 0.05$; * versus compared to that of non-treated control group.

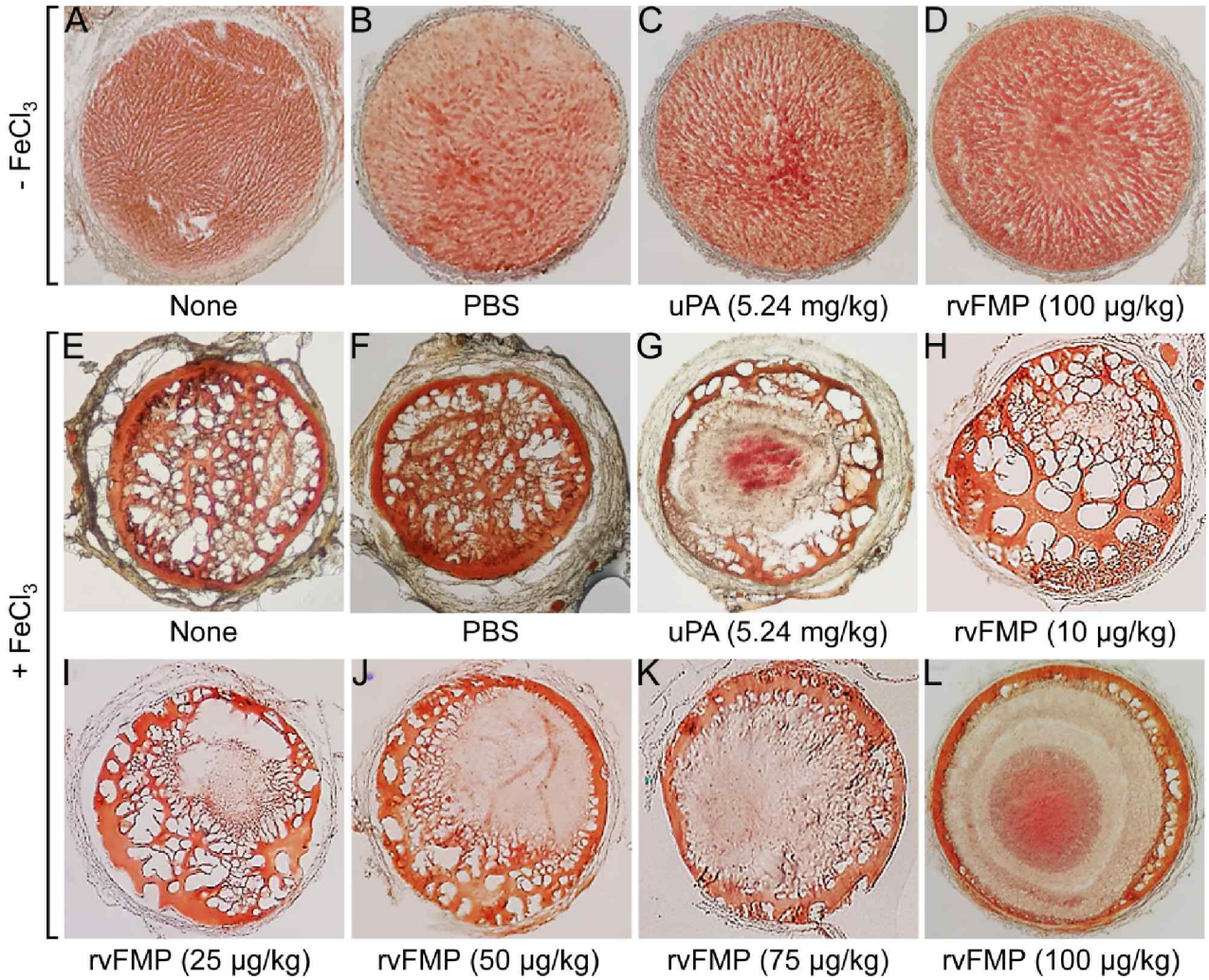

Fig. 23. Effect of rvFMP on $FeCl_3$-induced thrombus formation in rat carotid artery. (A-L) Rat tails were injected intravenously without (A) or with PBS (B and F), uPA (C and G), or various concentrations of rvFMP (D and H-L) as indicated. Ten min later, thrombi were induced without (A-D) and with 4% $FeCl_3$ (E-L) for 10 min in the right carotid arteries as described in Materials and methods. The micro-slices (20 μm in thickness) were then obtained by cryostat sectionings and the images were photographed.

that the rvFMP has an antithrombotic activity.

3-2-4. Effect of rvFMP on κ-carrageenan-induced thrombus formation in rat tail

The anti-thrombotic effect of rvFMP was also confirmed using κ-carrageenan-induced rat tail thrombosis model (Fig. 24) (Majumdar *et al*., 2016; Bekemeier *et al*., 1987; Ma *et al*., 2015). The vascular thrombi induced by the injection of 4 mg/kg of carrageenan decreased in amount depending on the treated with 5.24 mg/kg of uPA and various concentrations of rvFMP (25-100 μg/kg) (Fig. 24). Under the experimental condition, the lengths of rat tail thrombi induced by PBS and 5.24 mg/kg of uPA were estimated to be approximately 12.93 and 10.3 cm, respectively, and those by 25, 50, 75, and 100 μg/kg of rvFMP were found to be about 12.03, 10.48, 9.11, and 6.03 cm, respectively (Fig. 24A). These results indicate that the actual thrombus dissolution by 5.24 mg/kg of uPA is 20.39% and those by 25, 50, 75, and 100 μg/kg of rvFMP are 6.98, 18.94, 29.56, and 53.35%, respectively (Fig. 24B). The results suggest that the rvFMP can dissolve the blood clots formed by carrageenan.

3-2-5. Effect of uPA or rvFMP on bleeding time in mouse tail

The effect of rvFMP on bleeding time was investigated using the mouse tail bleeding model (Fig. 25). As shown in Fig. 25, uPA (5.24 mg/kg) and rvFMP (0.5 and 0.9 mg/kg) extended the bleeding time by 3.95 min and an average of 8.3 min, respectively, compared to the non-treated control (6.8 minutes). These results suggest that rvFMP may somewhat interfere with blood

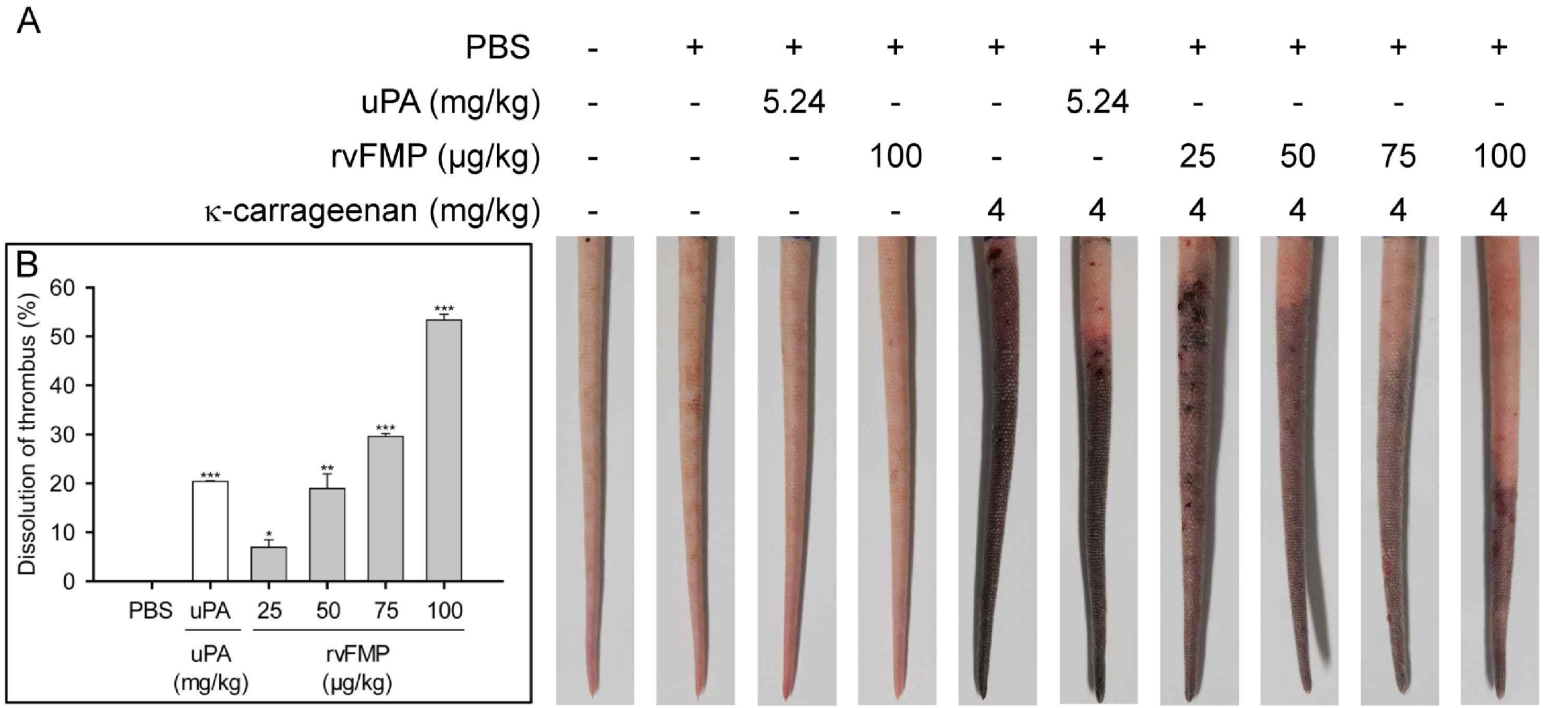

Fig. 24 . Effect of rvFMP on κ-carrageenan-induced thrombus formation in rat tail. (A) The thrombolytic activity of rvFMP *in vivo*. Rat tail was administered intravenously with PBS, uPA (5.24 mg/kg) or various concentrations of rvFMP as indicated. Ten min later, the thrombi were induced with 4 mg/kg of κ-carrageenan and photographed at 24 h. Symbols '+' and '-' represent the addition and the omission of the corresponding additive, respectively. (B) Relative dissolution of κ-carrageenan-induced thrombi by rvFMP. The thrombus length was measured from (A) and the dissolution of thrombus was calculated in percent as described in Materials and methods. *$p < 0.05$, **$p < 0.005$, and ***$p < 0.0005$ versus compared to that of PBS-dissolved κ-carrageenan-treated group.

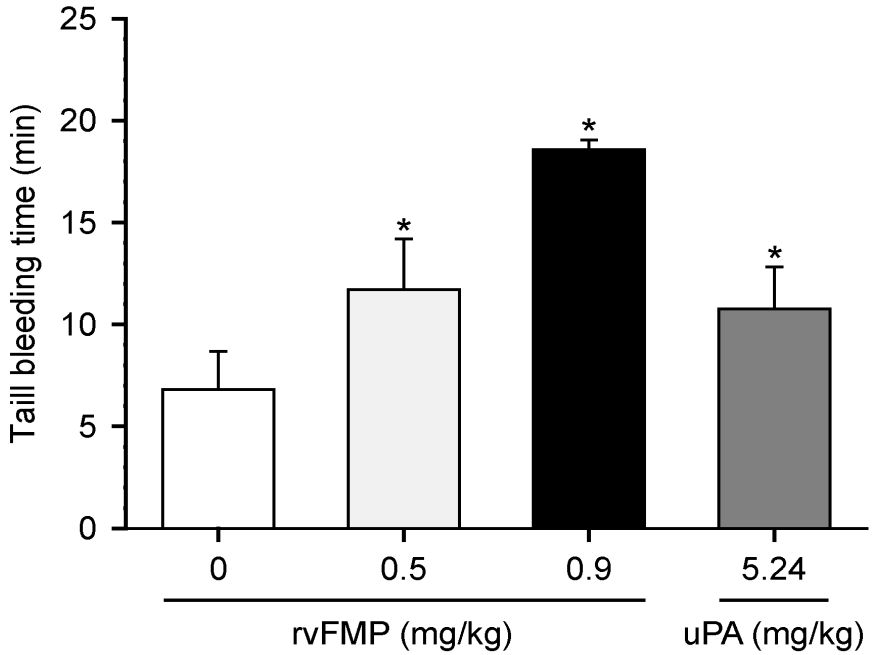

Fig. 25. Effect of uPA or rvFMP on bleeding time in mouse tail. BALB/c mice (n = 4 per group) were injected with various doses of rvFMP or uPA as indicated and the bleeding time was measured for 20 min as described in Materials and methods. *, $p < 0.05$ versus compared to that of non-treated control group.

clotting at doses over 0.5 mg/kg *in vivo*.

3-2-6. Artificial blood clot degradation by rvFMP

The blood clot degradation by rvFMP was verified by voluntary coagulation in test tube using fresh mouse blood (Fig. 26). The addition of rvFMP resulted in dose-dependent degradation of the blood clot. When rvFMP was treated at various concentrations (5, 10, and 15 μg), the solubilities of blood clots were 56.7, 58.6, and 67.4%, respectively (Table 5). However, 50% solubility of thrombosis was observed by 5 μg of plasmin. These results suggest that rvFMP has higher fibrin degradation activity than plasmin.

3-3. Effect of rvFMP on innate immune response

3-3-1. Effect of rvFMP on human zymogens involved in contact system

Contact system is widely involved in inflammatory response and autoimmune disease. It has been known for a long time that the activation of this system produces a potent pro-inflammatory non-peptide bradykinin through cleavage of HK by PK. Thus the contact system was also named plasma kallikrein-kinin system (Fedoseev *et al*., 1992). The ability of rvFMP to activate the zymogens involved in the intrinsic pathway of coagulation and the kallikrein/kinin system was first examined *in vitro* (Figs. 27-31). To confirm that the polypeptide fragments that can constitute the active enzyme are produced by rvFMP cleavage, 10 μg of zymogens (FXII, FXI, FX, and PPK) was digested with 0.2 μg for 1 or 5 min at 37°C and the result was analyzed on 12% SDS-polyacrylamide gel (Figs. 27-31). The polypeptide fragments comparable

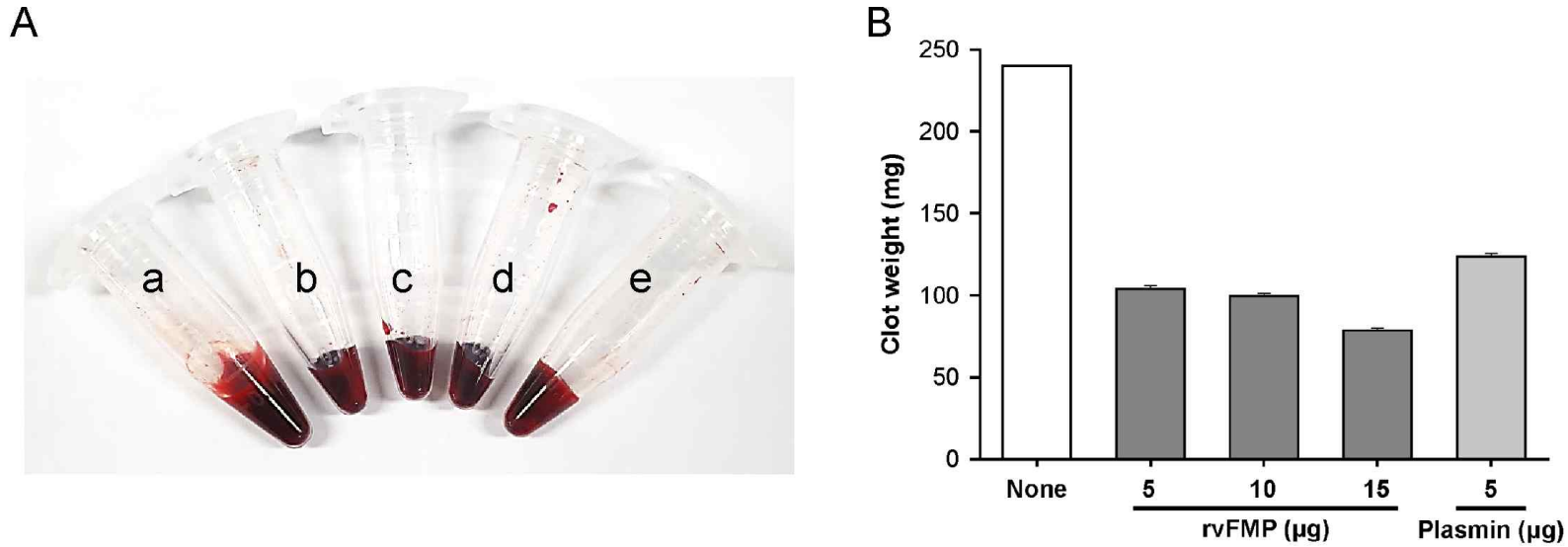

Fig. 26. Fibrinolytic effect of rvFMP on artificial blood clot. (A) Blood clot lysis assay. a, control; b, 5 μg rvFMP; c, 10 μg rvFMP; d, 15 μg rvFMP; e, 5 μg plasmin. (B) Comparison of *in vitro* blood clot lysis by various concentrations of rvFMP and plasmin. The residual thrombi were isolated and weighted after the treatments for 1 h at 37°C.

Table 5. Clot lysis of blood samples treated with different concentrations of rvFMP.

Sample	Thrombotic weight formed (mg)[a]	Residual thrombotic weight (mg)[b]	Degradation ratio (%)[c]
Control	240	240.0 ± 0.0	0.0 ± 0.0
rvFMP (5 μg)	240	104 ± 1.9	56.7 ± 0.8
rvFMP (10 μg)	240	99.5 ± 1.8	58.6 ± 0.8
rvFMP (15 μg)	240	78.6 ± 1.3	67.4 ± 0.2
Plasmin (5 μg)	240	123.6 ± 1.7	50.0 ± 0.7

[c]Inhibition ratio = (Weight[a] - Weight[b]) / Weight[a] x 100

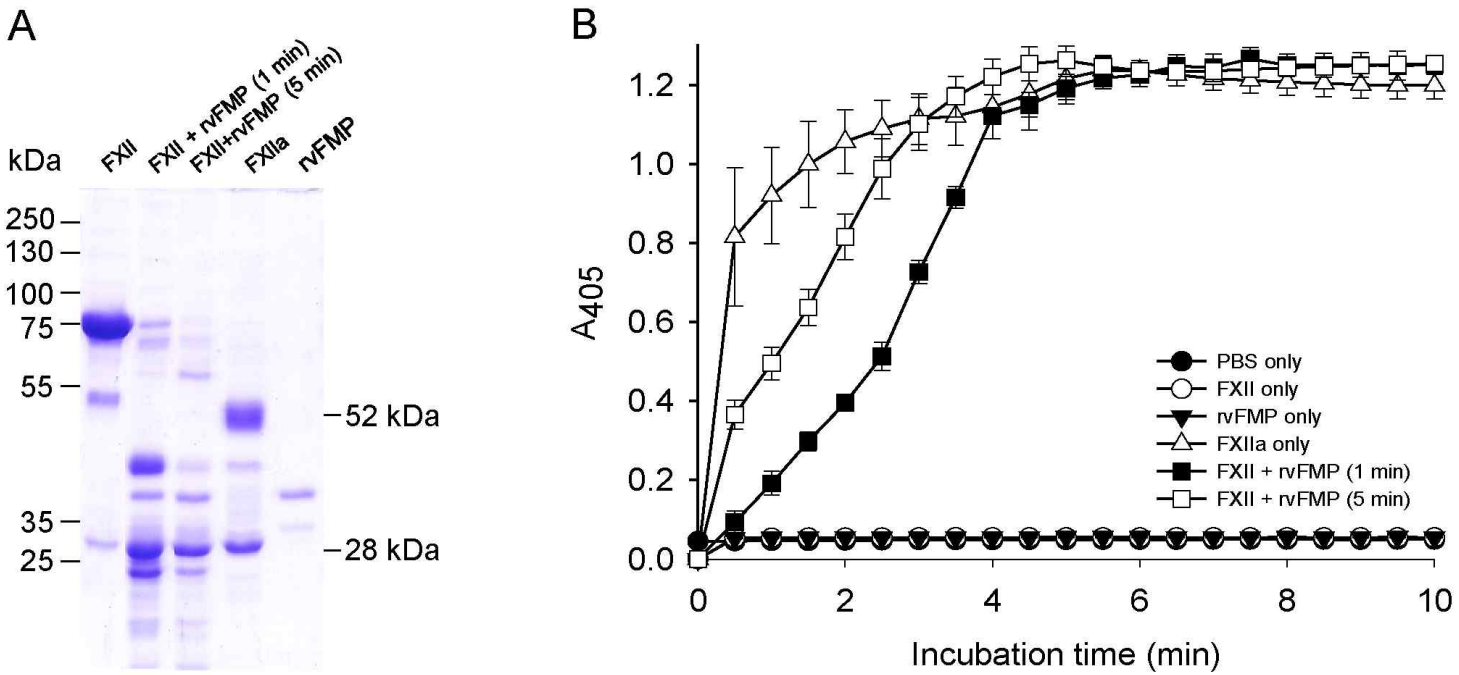

Fig. 27. Cleavage and activation of FXII by rvFMP. (A) FXII (10 μg) was cleaved with rvFMP (0.2 μg) at 37°C for 1 min or 5 min and the resulting products were analyzed on 12% SDS-polyacrylamide gel, together with FXIIa (5 μg) and rvFMP (0.2 μg). (B) FXII (5 μg) was cleaved with rvFMP (0.2 μg) at 37°C 1 min or 5 min, and then 1,10-PT (1 mM) was added to inhibit the rvFMP activity. Thereafter, the activities derived from rvFMP-cleaved zymogens were examined with 0.4 mM of S-2302. As a positive control, the activity of FXIIa (1 μg) was also analyzed under the same experimental condition. In the assay, amidolytic activity was measured every 30 s in A_{405} for 10 min at 37°C.

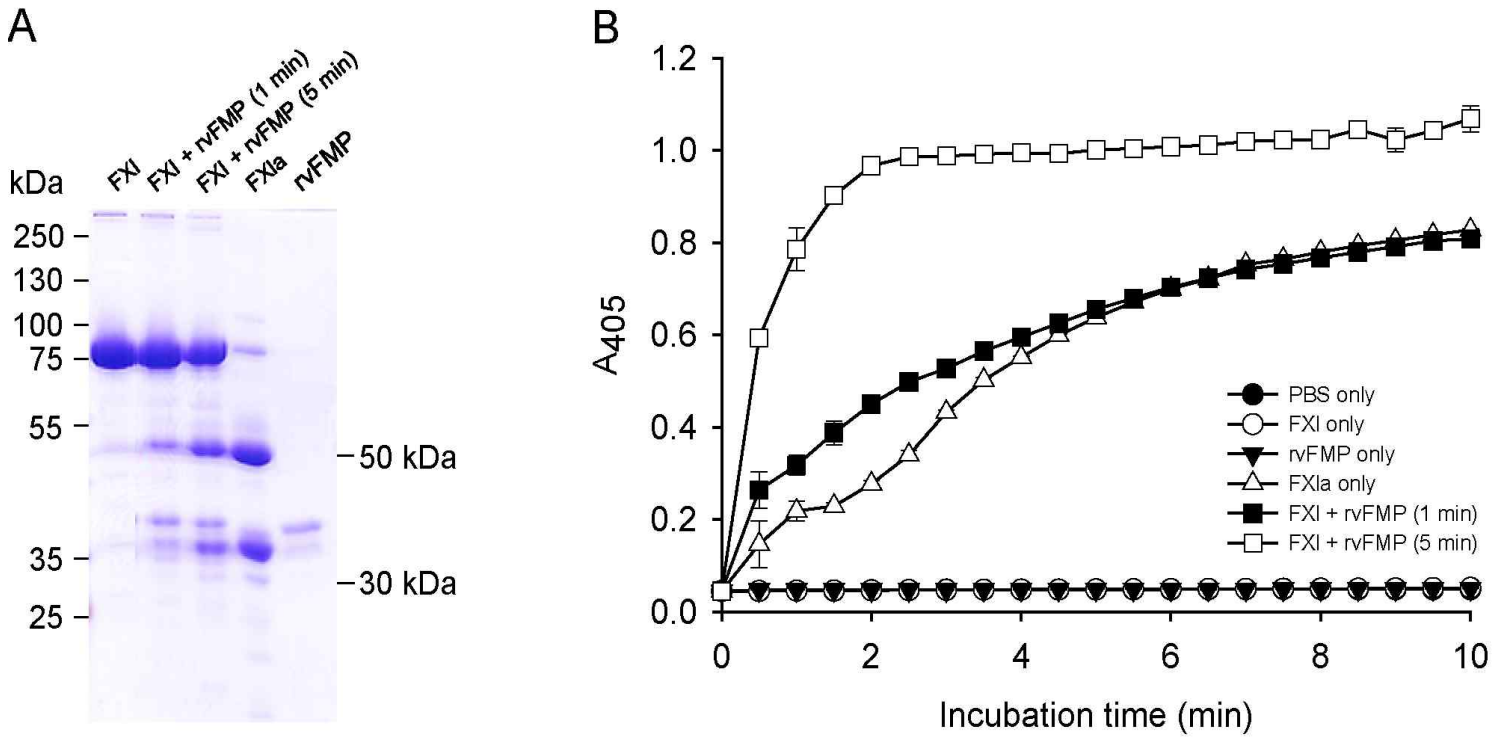

Fig. 28. Cleavage and activation of FXI by rvFMP. (A) FXI (10 μg) was cleaved with rvFMP (0.2 μg) at 37°C for 1 min or 5 min and the resulting products were analyzed on 12% SDS-polyacrylamide gel, together with FXIa (5 μg) and rvFMP (0.2 μg). (B) FXI (5 μg) was cleaved with rvFMP (0.2 μg) at 37°C 1 min or 5 min, and then 1,10-PT (1 mM) was added to inhibit the rvFMP activity. Thereafter, the activities derived from rvFMP-cleaved zymogens were examined with 0.4 mM S-2366. As a positive control, the activity of FXIa (1 μg) was also analyzed under the same experimental condition. In the assay, amidolytic activity was measured every 30 s in A_{405} for 10 min at 37°C.

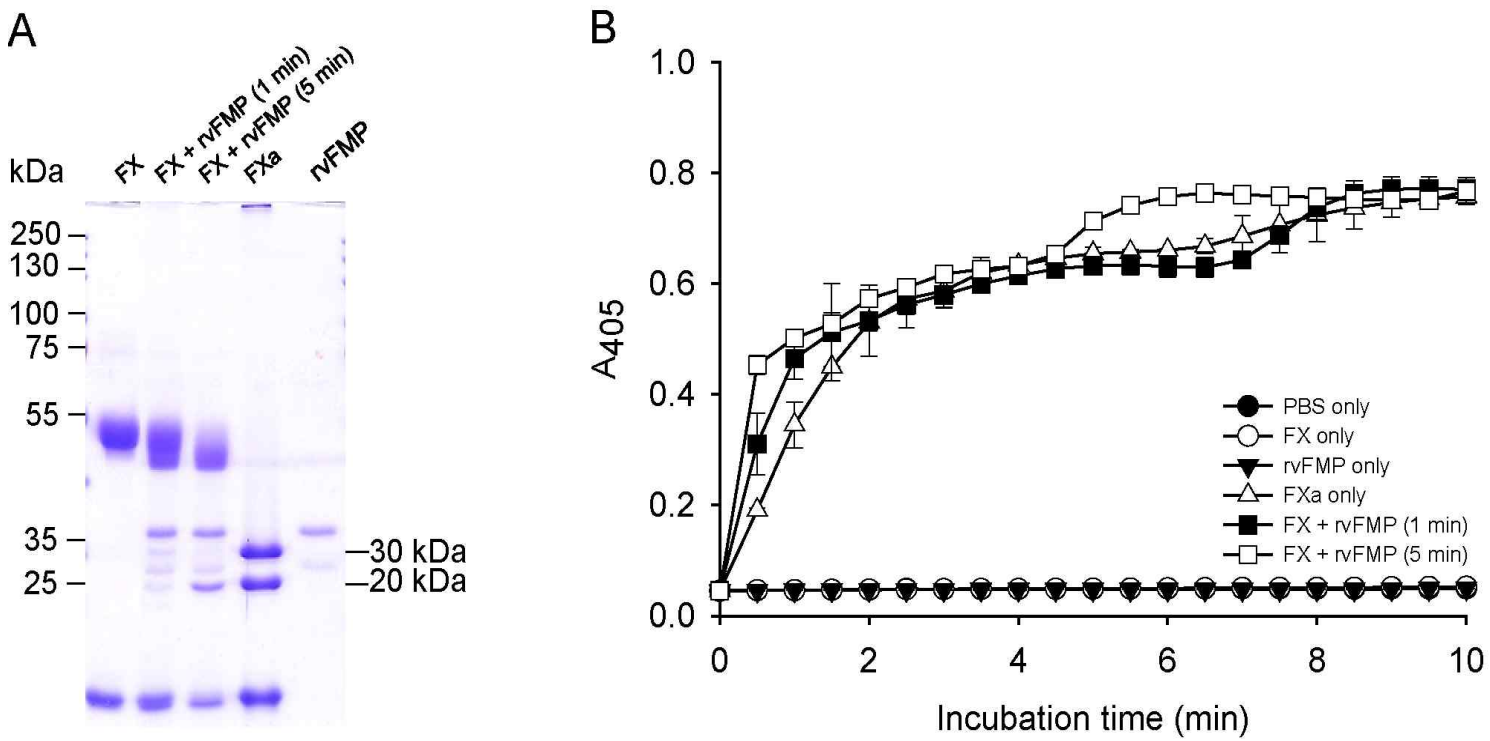

Fig. 29. Cleavage and activation of FX by rvFMP. (A) FX (10 μg) was cleaved with rvFMP (0.2 μg) at 37°C for 1 min or 5 min and the resulting products were analyzed on 12% SDS-polyacrylamide gel, together with FXa (5 μg) and rvFMP (0.2 μg). (B) FX (5 μg) was cleaved with rvFMP (0.2 μg) at 37°C 1 min or 5 min, and then 1,10-PT (1 mM) was added to inhibit the rvFMP activity. Thereafter, the activities derived from rvFMP-cleaved zymogens were examined with 0.4 mM S-2765. As a positive control, the activity of FXa (1 μg) was also analyzed under the same experimental condition. In the assay, amidolytic activity was measured every 30 s in A_{405} for 10 min at 37°C.

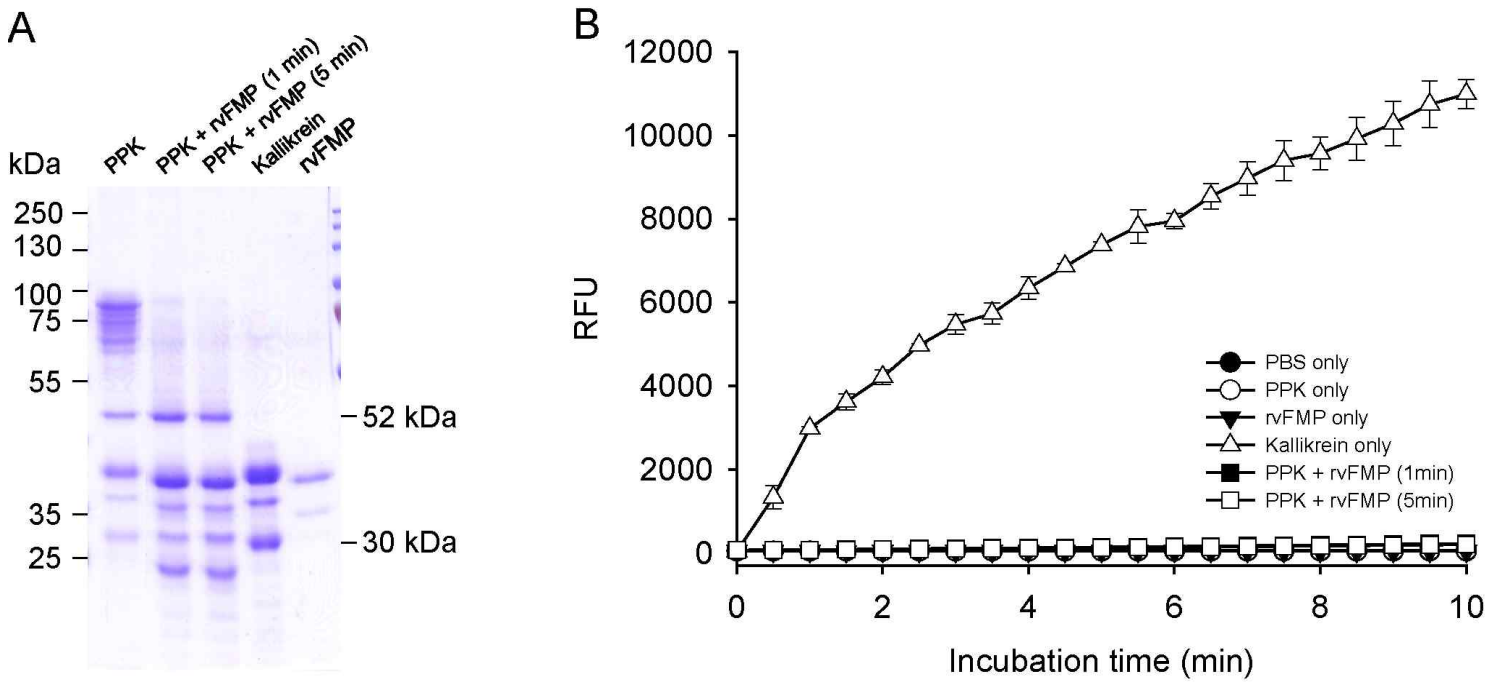

Fig. 30. Cleavage and activation of PPK by rvFMP. (A) PPK (10 μg) was cleaved with rvFMP (0.2 μg) at 37°C for 1 min or 5 min and the resulting products were analyzed on 12% SDS-polyacrylamide gel, together with Kall (5 μg) and rvFMP (0.2 μg). (B) PPK (5 μg) was cleaved with rvFMP (0.2 μg) at 37°C 1 min or 5 min, and then 1,10-PT (1 mM) was added to inhibit the rvFMP activity. Thereafter, the activities derived from rvFMP-cleaved zymogens were examined with 0.4 mM H-D-Val-Leu-Arg-AFC. As positive controls, the activities of the Kall (1 μg) was also analyzed under the same experimental condition. The fluorescence was also monitored every 30 s at λ_{ex} = 400 nm and λ_{em} = 505 nm for 10 min at 37°C, in which the activity was expressed as the relative fluorescence unit (RFU).

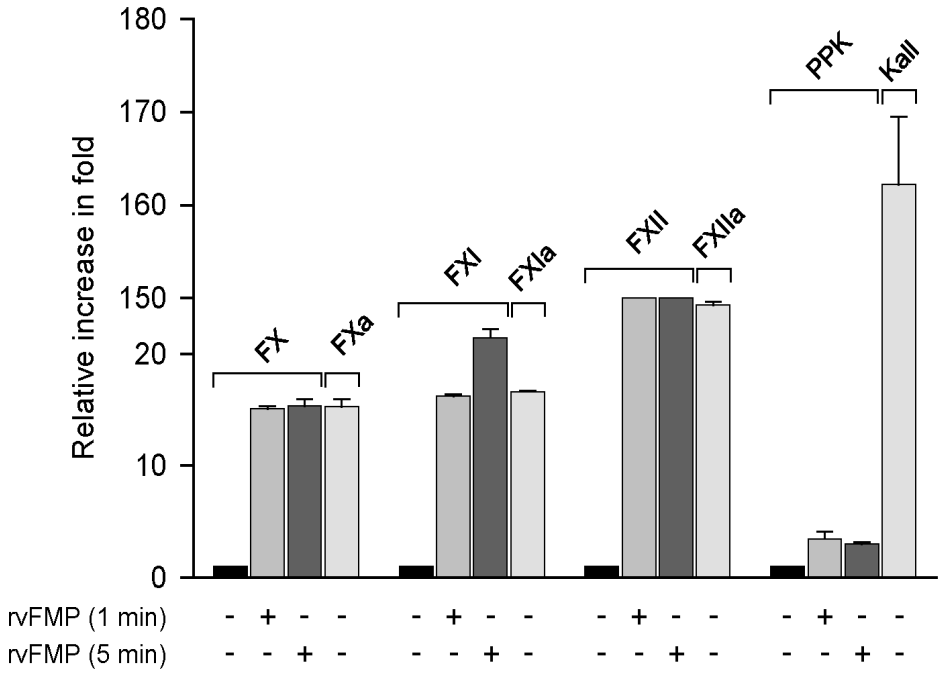

Fig. 31. Cleavage and activation of human zymogens involved in the contact system by rvFMP. The enzyme activities derived from rvFMP-cleaved zymogens were calculated, for which the mean values ± S.D. of three independent experiments at the incubation periods of 10 min were expressed as relative increases in fold, compared to that of rvFMP-nontreated control.

sizes to the chains comprising native enzymes seemed to be produced by rvFMP cleavage from the corresponding zymogens (Figs. 27-30). These results suggest that rvFMP may activate the zymogens through proteolysis. Based on these results, the actual zymogen activation ability of rvFMP was examined *in vitro* using chromogenic or fluorogenic peptide substrates specific for the activated enzymes (Figs. 27-30). As shown in Fig. 27B, there was a clear increase in absorbance at 405 nm when 5 μg of FXII was digested with 0.2 μg of rvFMP at 37°C for 1 or 5 min and then 0.4 mM of S-2302 was added as a substrate, with no increase with zymogen only or rvFMP alone. The relative FXIIa activity derived from rvFMP-cleaved FXII increased to an average of 25.5-folds, compared to that of non-cleaved zymogen (Fig. 31). These results suggest that rvFMP can activate FXII to active FXII by proteolysis. The ability of rvFMP to activate, other zymogens including FXI, FX, and Kall under the same experimental condition (Figs. 27-31). When S-2302 for FXIa (Fig. 28B), S-2765 for FXa (Fig. 29B), or H-D-Val-Leu-Arg-AFC for Kall (Fig. 30B) was used as a substrate for assaying rvFMP-induced activity, the relative fold increases were found to be 21.5 from FXI, 15.1 from FX, and 2.96 from PPK (Fig. 31). These results suggest that rvFMP exhibits a proteolytic activity to activate the zymogens involved in the intrinsic pathway of coagulation, but not activate kallikrein/kinin system.

3-3-2. Effect of rvFMP on the activation of blood contact system

The results obtained from *in vitro* experiments showed that rvFMP could convert components of the contact system to the active forms of enzymes except for PPK. Therefore, it was needed to confirm if rvFMP could activate the zymogens present in the plasma. To examine the ability, 10% of blood plasma

was treated with 1 μg of rvFMP for 1 or 5 min and the induced activities of contact system components were observed with 0.4 mM each of synthetic peptide substrates specific for the activated zymogens (Figs. 32-35). When S-2302 was added to the rvFMP-treated plasma, the total activity of FXIIa and FXIa increased to an average of 2.21 and 3.06-folds, compared to that of the substrate added only (Fig. 36). However, a background level of the increase could be observed with the same substrate when the enzyme was co-incubated with 1,10-PT, a potent inhibitor of rvFMP (Figs. 32 and 33), suggesting that the increase of amidolytic activity is directly related to the rvFMP-cleaved activation of FXII and FXI zymogens. Likewise, rvFMP also could activate other plasma zymogens, such as FX (Fig. 34) and PPK (Fig. 35), in which the fold-increases of FXa and Kall activities were found to be 2.24 and 1.09, respectively, compared to those of their corresponding substrates only added (Fig. 31). However, the activations were leveled down, compared to those *in vitro* because the rvFMP activity must have been inhibited by physiological inhibitors such as α2-macroglobulin present in plasma (Chang *et al.,* 2005). The rvFMP could convert inactive plasma FXII, FXI, and FX zymogens to active FXIIa, FXIa, and FXa, respectively, plasma milieu except for PPK. Kallikrein not only cleaves HMWK, generating bradykinin, but also cleaves several complement proteins including C3, C5 and factor B. However, rvFMP could not evoke an inflammatory reaction of the kallikrein/Kinin system because it could not activate kallikrein.

3-3-3. Effect of rvFMP on complement system activation

The complement system is integral to innate immunity and shares numerous interactions with components of the haemostatic pathway, helping to

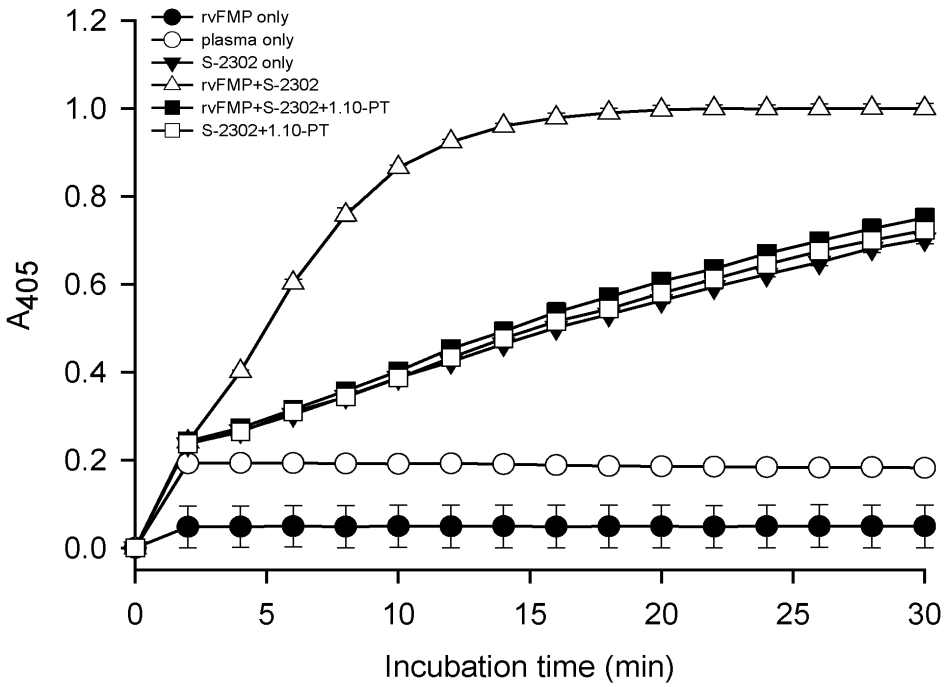

Fig. 32. rvFMP-induced activation of FXII in plasma milieu. Blood plasma (10%) was mixed with rvFMP (1 μg) in the absence or presence of 1,10-PT (1 mM) and 0.4 mM of S-2302. The amidolytic activities were monitored every 2 min for 30 min at 37°C by measuring A_{405}.

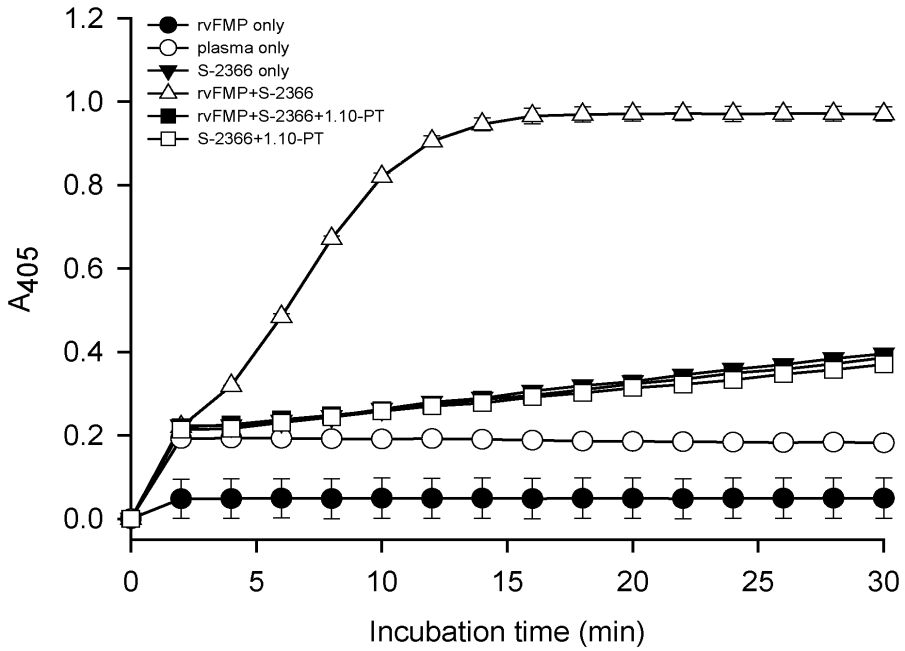

Fig. 33. rvFMP-induced activation of FXI in plasma milieu. Blood plasma (10%) was mixed with rvFMP (1 μg) in the absence or presence of 1,10-PT (1 mM) and 0.4 mM of S-2366. The amidolytic activities were monitored every 2 min for 30 min at 37°C by measuring A_{405}.

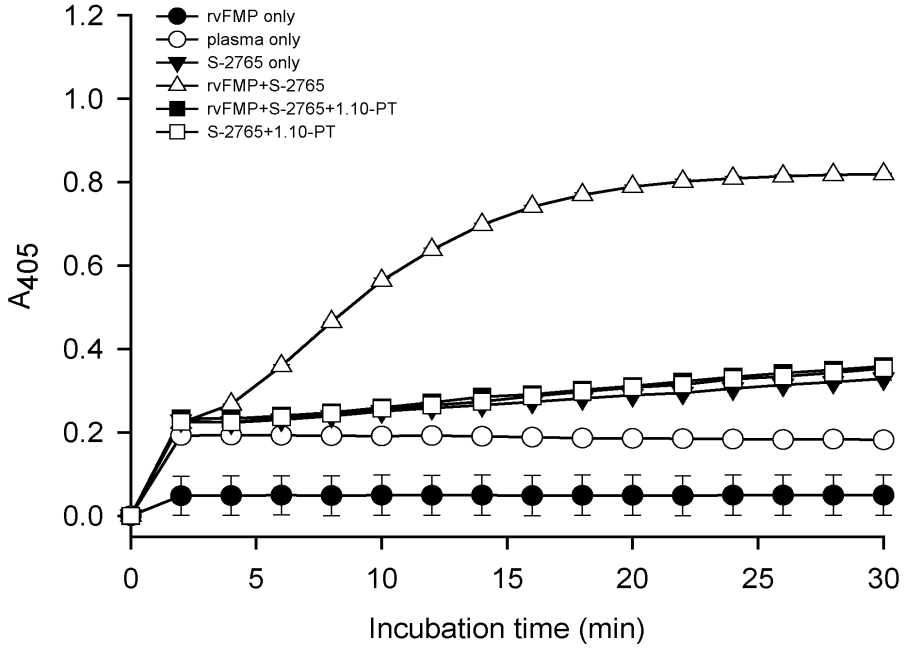

Fig. 34. rvFMP-induced activation of FX in plasma milieu. Blood plasma (10%) was mixed with rvFMP (1 μg) in the absence or presence of 1,10-PT (1 mM) and 0.4 mM of S-2765. The amidolytic activities were monitored every 2 min for 30 min at 37°C by measuring A_{405}.

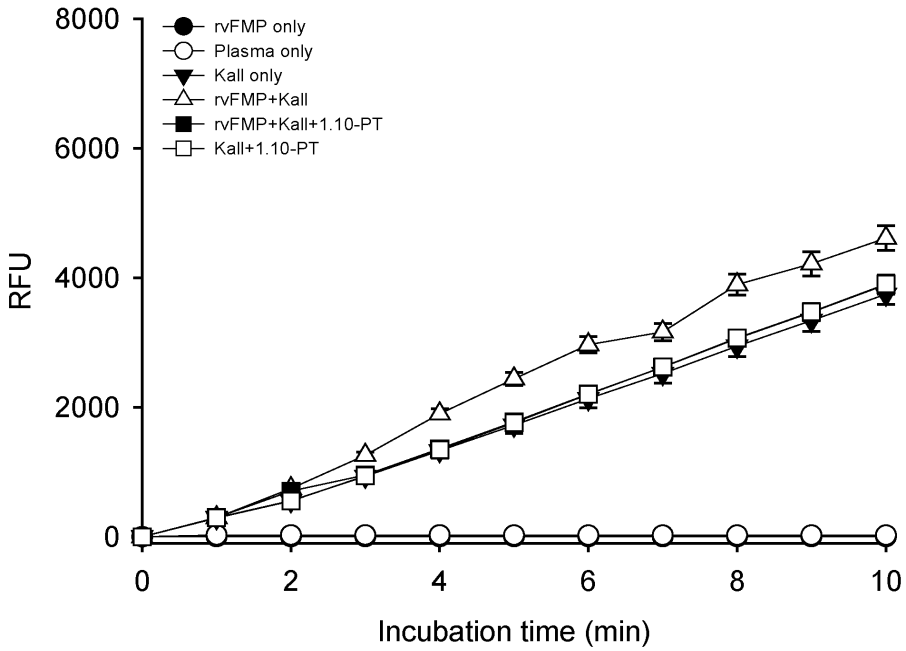

Fig. 35. rvFMP-induced activation of PPK in plasma milieu. Blood plasma (10%) was mixed with rvFMP (1 μg) in the absence or presence of 1,10-PT (1 mM) and 0.4 mM of H-D-Val-Leu-Arg-AFC. The fluorescence produced was monitored every 2 min for 10 min at 37°C by measuring λ_{ex} = 400 nm and λ_{em} = 505 nm.

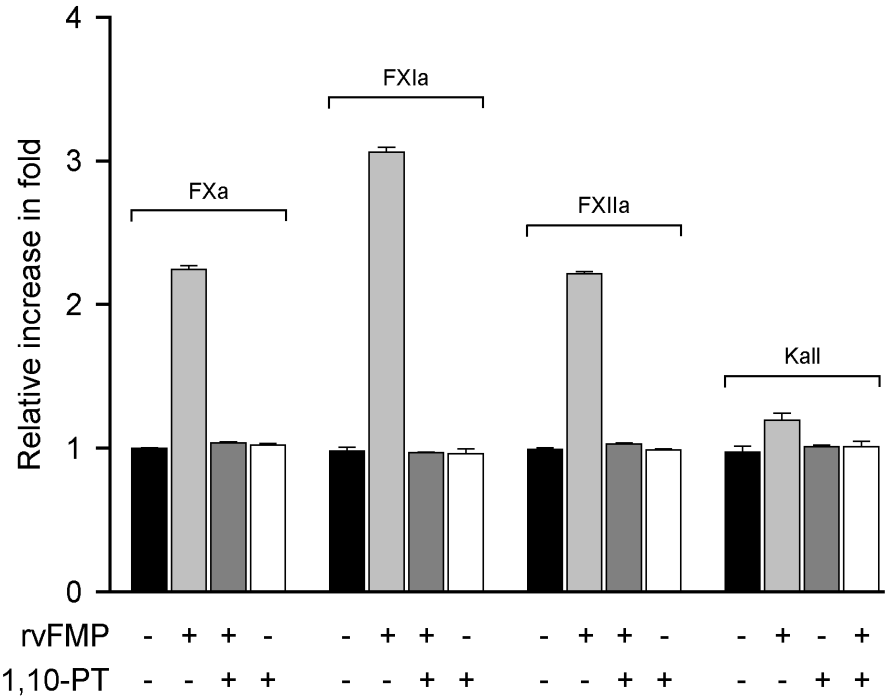

Fig. 36. rvFMP-induced activation of contact system components in plasma milieu. The enzyme activities derived from rvFMP-reacted plasma were calculated, for which the mean values ± S.D. of two independent experiments at the incubation periods of 10 min were expressed as relative increases in fold, compared to that of rvFMP-nontreated control.

maintain physiological equilibrium. The complement system can be activated via three traditional pathways. The classical pathway (antigen: antibody complexes on pathogen surfaces), mannose-binding lectin pathway (binding of mannan-binding lectin, a serum protein, to mannose-containing carbohydrates on the surface of bacteria or viruses) and the constitutively active alternative pathway (initiated when a spontaneously activated complement component binds to the pathogen surface). Each pathway, despite the different mechanisms of activation, ultimately converges to generate the central protease C3 convertase. C3 convertase has further downstream actions; generating the potent anaphylatoxins C3a and C5a as well as the membrane attack complex (MAC), C5b-9, which serve pivotal roles in inflammation and the creation of transmembrane channels within infected cellular membranes leading to cell lysis and death respectively (Janeway *et al.,* 2001; Huber-Lang *et al*., 2006; Arachchillage *et al.,* 2016). To examine the ability of rvFMP to activate the complement system in plasma, 10% of human plasma was treated with rvFMP (10, 20, 30, or 40 ng) for 3 min at 37°C and subjected to Western blot analysis (Figs. 37-39). As shown in Figs. 37-39, the complement molecule C4a, C3a, and C5a were not produced from C4, C3, and C5 by rvFMP. These results suggest that rvFMP could not convert plasma C3, C4, and C5 to their respective active factors.

3-3-4. Effect of rvFMP on inflammatory response in Raw 264.7 cells

It has been known that the inflammatory response and innate immunity are closely related to each other, together with blood coagulation (Keragala *et al.,* 2018). Blood clot formation is a prime example of the innate immunity's efforts to minimize infection, an inherent complication of wounds and

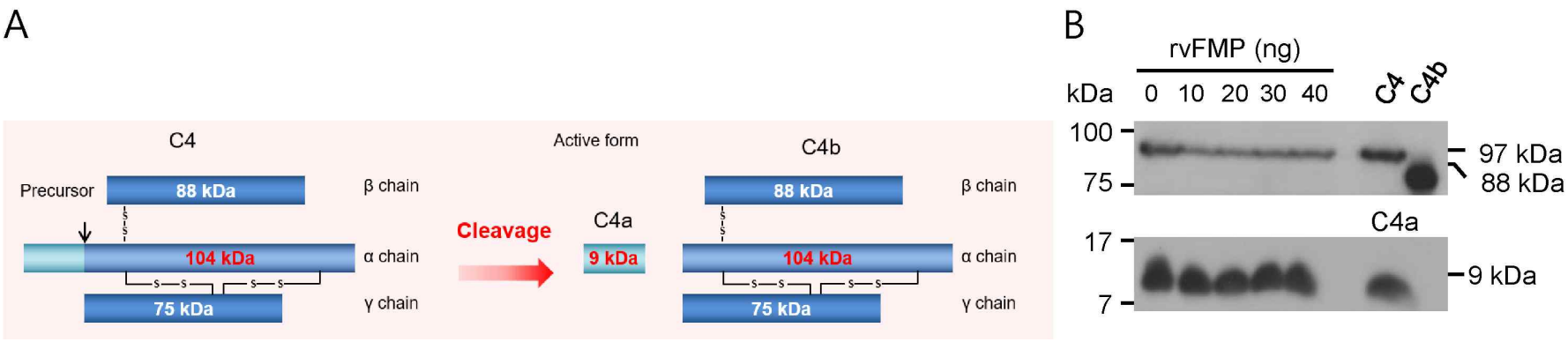

Fig. 37. Cleavage of complement C4 by rvFMP in plasma. (A) Schematic diagram for the activation of C4. (B) Human blood plasma (10%) was incubated with rvFMP (0-40 ng) for 3 min at 37°C and the resulting products were separated by SDS-PAGE and Western blotting was performed using anti-C4 antibody or anti-C4a antibody.

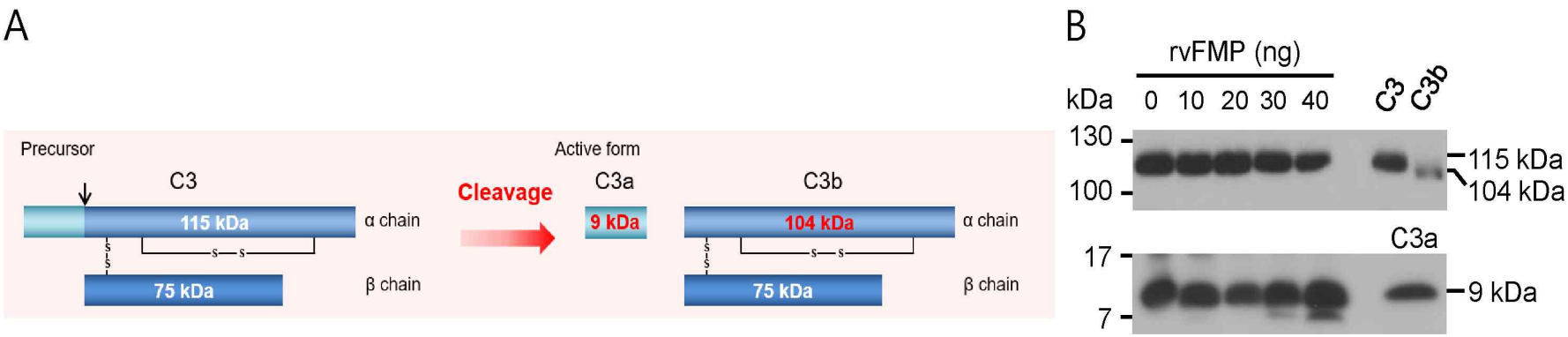

Fig. 38. Cleavage of complement C3 by rvFMP in plasma. (A) Schematic diagram for the activation of C3. (B) Human blood plasma (10%) was incubated with rvFMP (0-40 ng) for 3 min at 37°C and the resulting products were separated by SDS-PAGE and Western blotting was performed using anti-C3 antibody or anti-C3a antibody.

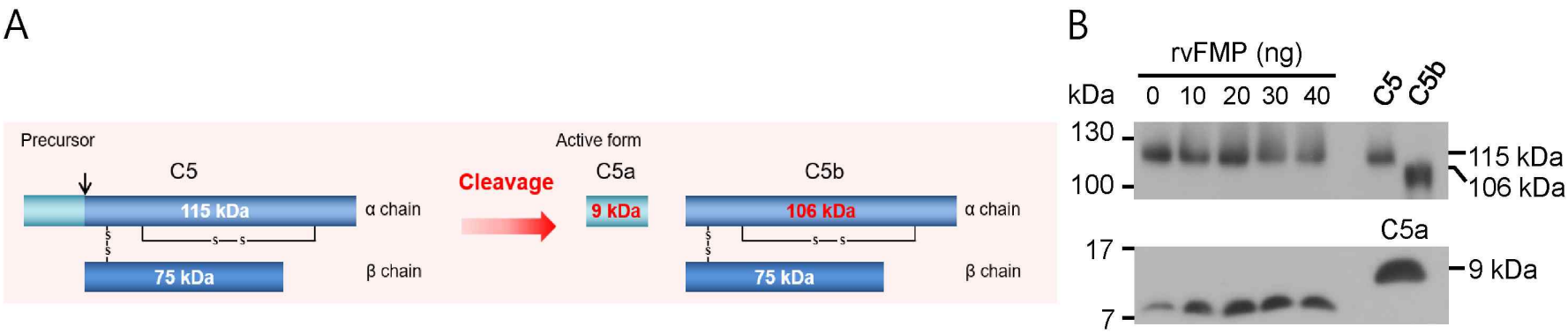

Fig. 39. Cleavage of complement C5 by rvFMP in plasma. (A) Schematic diagram for the activation of C5. (B) Human blood plasma (10%) was incubated with rvFMP (0-40 ng) for 3 min at 37°C and the resulting products were separated by SDS-PAGE and Western blotting was performed using anti-C5 antibody or anti-C5a antibody.

injuries. In addition, there are well-described changes in the inflammatory response in patients with acute ischaemic cerebrovascular stroke and acute myocardial infarction (Anrather & Iadecola, 2016; Horvath *et al.,* 2016). Similarly, many invading bacteria have evolved a means to combat host defences by generating antithrombotic and pro-fibrinolytic enzymes to remove restrictive thrombi and achieve pathogen dissemination in the host. Although rvFMP shows a clear arterial thrombolytic capability (Figs. 23 and 24) with its proteolytic ability to digest blood clots (Fig. 20), there may be concerns that the injection of rvFMP *in vivo* can provoke cytotoxicity, bleeding and/or inflammatory response. However, results from MTT analysis (Stepanenko *et al.,* 2015) and ELISA (Kaiser *et al.,* 2018) showed that rvFMP does not exhibit cytotoxicity, up to 20 μg/ml (data not shown) and could not induce tumour necrosis factor-alpha. TNF-α is one of the typical cytokines involved in the inflammatory response of Raw 264.7 cells (Fig. 40). These results suggest that the rvFMP could not induce an inflammatory response because it does not produce TNF-α.

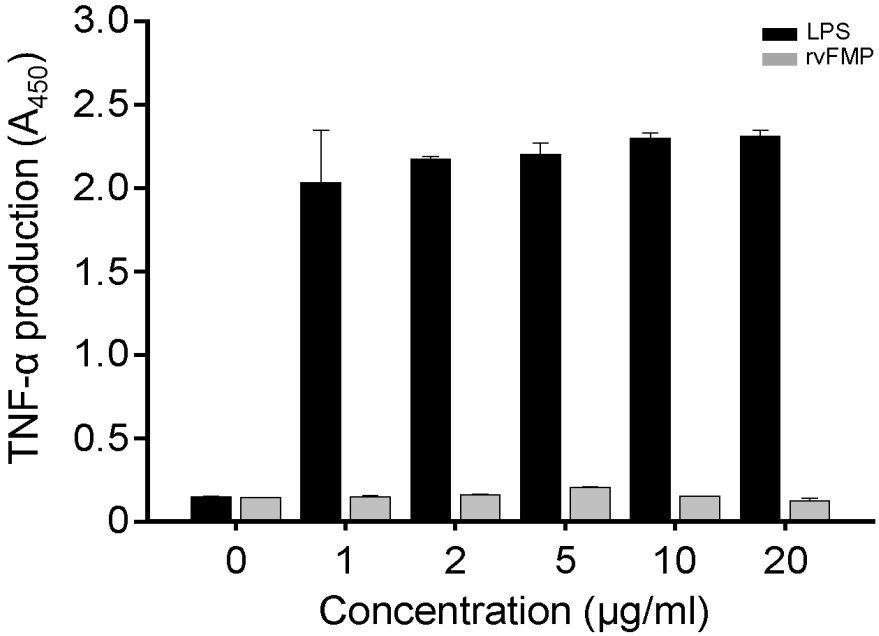

Fig. 40. Effects of rvFMP and lipopolysaccharide (LPS) on the induction of tumour necrosis factor-alpha (TNF-α) in Raw 264.7 cells. Cells were treated for 3 h with various concentrations of rvFMP or LPS as indicated and the cell extracts were prepared as described elsewhere. The production level of TNF-α was measured using ELISA kit for TNF-α, in which the absorbance at 450 nm was examined. Data are expressed as mean S.E.M. of triplicates.

4. 적 요

인간 혈장 및 쥐 혈전증 모델에서 재조합 단백질분해효소 rvFMP의 혈전용해 특성에 관한 연구

임 도 성
지도교수 : 이 정 섭
조선대학교 대학원
글로벌바이오융합학과

심혈관계 질환은 전 세계적으로 주요 사망원인 중 하나이며, 주로 동맥에 남아있는 피브린 침착물(fibrin clot)에 의해 유발될 수 있다. 현재 urokinase(uPA), streptokinase 및 tissue-type plasminogen activator(tPA)와 같은 효소들이 혈전 용해제로 임상에서 사용되고 있지만, 이들 모두는 plasminogen을 plasmin으로 활성화시켜 혈관 내의 혈전을 분해하게 하는 간접작용 효소이며, 이들은 종종 출혈, 저혈압, 메스꺼움 및 알레르기 반응과 같은 부작용을 동반한다. 본 연구는 혈관 내 혈전에 직접 작용하여 분해함으로써 부작용이 적은 새로운 혈전 용해효소를 개발하고자 수행되었다. 본 연구에 사용된 *Vibrio furnissii*균은 위장염 및 피부병변을 일으킬 수 있는 해양세균이며, 전체 유전체서열은 2011년에 결정된 바 있다. 이 미생물은 자외선 차단을 위한 피부 관리, 항생제 대체재, 식품 보존제 등의 활성성분으로 사용할 수 있는 엑토인, 박테리오신 등, 다양한 2차 대사물을 생산한다. 일반적으로 여러 종류의 비브리오 균주는 피브리노겐(fibrinogen)과 피브린(fibrin)을 분해 할 수 있는 다양한 종류의 단백질분해효소(protease)를 분비하는 것으로 알려져 있다. 그러나 혈전분해제 개발 측면에서 *V. furnissii*에서 생성되는 분비성 단백질분해효소에 대한 연구는 전무하다. 본 연구실에서는 *V. furnissii*는 vFMP(*V. furnissii* metalloprotease의 약자)라 명명한 44 kDa 크기의 metalloprotease를 분비한다는 사실을 밝혀낸 바 있다. 본 연구에서는 *V. furnissii* KCCM41679 균주의 유

전체 DNA로부터 중합효소연쇄반응(polymerase chain reaction, PCR)을 이용하여 *vFMP* 유전자를 클로닝한 후, 대장균에서 발현시켜 재조합 단백질분해효소를 분리·정제하였으며 이를 rvFMP(recombinant vFMP)라 명명하였다. 클로닝한 *rvFMP* 유전자의 염기서열을 분석한 결과, 이 유전자는 1,827개의 nucleotide로 구성된 한 개의 열린 읽기틀(open reading frame, ORF)을 가지고 있으며, 이 ORF는 608개의 아미노산으로 이루어진 분자량, 약 67443.71 Da 크기의 단백질을 암호화할 수 있음을 확인하였다. 또한 이 유전자의 시작 및 종결 코돈은 각각 ATG 및 TAA인 것을 확인하였다. 염기서열로부터 유추한 rvFMP의 아미노산 서열을 다른 비브리오 균주들, 즉 *V. fluvialis*, *Vibrio* sp. RC586, *V. anguillarum*, *V. mimicus* 및 *V. vulnificus* 등이 분비하는 5종의 단백질분해효소의 아미노산 서열들과 비교분석한 결과, 평균 80.8%의 서열 유사성이 있음을 확인하였다. 이러한 결과는 이 효소들은 잘 보존된 단백질분해효소임을 시사하는 것이다. 아미노산 서열의 비교 분석을 통해, rvFMP는 608개의 아미노산으로 이루어진 prepro-rvFMP로 생성되며, 이는 신호서열(24개의 아미노산으로 구성), propeptide 부위(173개의 아미노산으로 구성) 및 Zn^{2+}-binding motif(HEXXHG-X_{18}-E)를 지닌 촉매 영역(411개의 아미노산으로 구성)으로 이루어져 있음을 확인하였다. 본 연구에서는 또한 *E. coli*에서 발현시킨 rvFMP 단백질분해효소를 2가지 음이온 크로마토그래피(HiTrap Q FF 및 Source 15 Q 4.6/100 PE 컬럼)와 단일 크기 배제 크로마토그래피(Superdex 75 10/300 GL 겔 여과 컬럼)를 순서대로 사용하여 정제하였다. SDS-PAGE로 확인한 결과, 정제한 rvFMP의 분자량은 약 44 kDa(rvFMP-44로 명명) 및 39 kDa(rvFMP-39로 명명) 크기를 임을 알 수 있었다. 이 두 효소의 N-말단 아미노산 서열을 분석한 결과, rvFMP-44는 N-AEATGTGP-C 서열을, rvFMP-39는 N-SGTTAYSY-C 서열을 N-말단에 지니고 있었다. 이러한 결과는, 전구체효소(zymogen)인 prepro-rvFMP의 N-말단 신호서열과 propeptide 부위가 세포외 분비 과정에서 잘려나가 활성화 효소인 rvFMP-44가 생성되며, 효소의 분리과정에서 N-말단의 51개 아미노산이 추가적으로 rvFMP-44로부터 자가분해(autolysis)에 의해 떨어져 나가 rvFMP-39가 생성됨을 시사하는 것이다. Azocasein을 기질로 확인한 결과, rvFMP 효소활성의 최적

pH와 온도는 각각 7.0 및 50°C임을 확인하였다. 또한 rvFMP의 단백질분해 활성은 1,10-phenanthroline(1,10-PT)와 ethylene glycol *bis*(2-aminoethyl ether) tetraacetic acid(EGTA) 등에 의해서는 억제되었으나, phenylmethylsulfonyl fluoride (PMSF)와 diisopropyl fluorophosphate(DFP)에 의해서는 억제 되지 않았다. 이러한 결과는 rvFMP가 전형적인 metalloprotease임을 시사하는 것이다. rvFMP는 bovine serum albumin(BSA), fibrinogen, prothrombin, collagen type IV, plasminogen 등과 같은 혈장 단백질들을 분해할 수 있었으며, γ-globulin은 거의 자르지 못하였다. rvFMP는 또한, 시험관 내에서 피브리노겐 및 피브린을 효과적으로 분해함을 확인하였으며, SDS-PAGE를 이용한 절단시험(cleavage assay)과 탁도 시험(turbidity assay)을 통해 분석한 결과, rvFMP는 피브리노겐의 Aα와 Bβ 사슬을 1분 이내에 완전히 절단하고, 피브린 중합체(fibrin polymer)를 효과적으로 분해함을 확인하였다. 또한 rvFMP는 교차-연결 피브린(cross-linked fibrin, XL-fibrin)도 절단할 수 있음을 SDS-PAGE를 통해 확인하였고, plasmin 보다 약 2.5배 더 강한 XL-피브린 절단 활성을 지니고 있음을 피브린 평판시험(fibrin plate assay)을 통해 확인하였다. 본 연구에서는 또한 $FeCl_3$에 노출시켜 혈관 혈전증을 유발시킨 쥐 경동맥과 kappa-carrageenan을 처리하여 혈전증을 유발시킨 쥐꼬리에서 항-혈전증에 대한 rvFMP의 효과를 분석하였다. 대조군으로 phosphate buffered saline(PBS), uPA(5.24 mg/kg), rvFMP(100 μg/kg)를 처리한 경우, 쥐의 경동맥에 혈전이 거의 형성되지 않았으나 $FeCl_3$에 노출시킬 경우, 광범위한 경동맥 혈전증이 유발되었다. 그러나 다양한 농도의 rvFMP(10-100 μg/kg)를 선 처리한 후, $FeCl_3$로 경동맥 혈전증을 유발시킨 경우에는 혈전형성이 농도-의존적으로 감소됨을 확인하였다. 이러한 rvFMP의 항-혈전 활성(anti-thrombotic activity)은 카라기난(carrageenan)-유도 쥐꼬리 혈전증 모델에서도 확인하였다. 카라기난(4 mg/kg)을 처리하여 혈관에 혈전을 형성을 유도한 후, uPA(5.24mg/kg) 또는 다양한 농도의 rvFMP(25-100 μg/kg)를 처리하였을 때, 혈관의 혈전이 농도-의존적으로 감소하였다. 이러한 결과들은 rvFMP가 생체 내에서도 혈관 혈전을 분해할 수 있는 효소활성을 지니고 있음을 시사하는 것이다. 본 연구에서는 또한 rvFMP(1.5 mg/kg)는 생쥐에서 내부 출혈을

유발하지 않으며, 혈장 내 피브리노겐의 농도를 크게 감소시키지 않을 뿐만 아니라 대식세포(Raw 264.7)에서 종양 괴사 인자-α(TNF-α)의 생성도 유도하지 않음을 확인하였다. 본 연구에서 얻은 결과를 종합할 때 rvFMP가 새로운 직접-작용 혈전용해제로 개발될 수 있는 가능성을 지닌 후보 효소임을 알 수 있다.

5. REFERENCES

Adkins JN, Varnum SM, Auberry KJ, Moore RJ, Angell NH, Smith RD, Springer DL, Pounds JG. Toward a human blood serum proteome: analysis by multidimensional separation coupled with mass spectrometry, Mol. Cell. Proteomics 2002; 1(12): 947-955.

Akazawa SI, Tokuyama H, Sato S, Watanabe T, Shida Y, Ogasawara W. High-pressure tolerance of earthworm fibrinolytic and digestive enzymes, J. Biosci. Bioeng. 2018; 125(2): 155-159.

Amarant T, Burkhart W, LeVine H, Arocha-Pinango CL, Parikh I. Isolation and complete amino acid sequence of two fibrinolytic proteinases from the toxic *Saturnid* caterpillar *Lonomia achelous,* Biochim. Biophys. Acta. 1991; 1079(2): 214-221.

Anderson L, Anderson NG. High resolution two-dimensional electrophoresis of human plasma proteins, Proc. Natl. Acad. Sci. U. S. A. 1977; 74(12): 5421-5425.

Arnold AE, Simoons ML. Thrombolytic therapy for evolving myocardial infarction needs an approach that integrates benefit and risk, Eur. Heart. J. 1995; 16(11): 1502-1509.

Arachchillage DR, Mackie IJ, Efthymiou M, Chitolie A, Hunt BJ, Isenberg DA, Khamashta M, Machin SJ & Cohen H. Rivaroxaban limits complement activation compared with warfarin in antiphospholipid syndrome patients with venous thromboembolism, J. Thromb. Haemost. 2016; 14 (11): 2177–2186.

Assakura MT, Reichl AP, Mandelbaum FR. Isolation and characterization of five fibrin(ogen)olytic enzymes from the venom of *Philodryas olfersii* (green snake), Toxicon 1994; 32(7): 819-831.

Avecilla ST, Ferrell C, Chandler WL, Reyes M. Plasma-diluted thrombin time to measure dabigatran concentrations during dabigatran etexilate therapy, Am.

J. Clin. Pathol. 2012; 137(4): 572-574.

Barthel LK, Raymond PA. Improved method for obtaining 3-microns cryosections for immunocytochemistry, J. Histochem. Cytochem. 1990; 38(9): 1383-38.

Ballal M, Shetty V, Bangera SR, Prabhu M, Umakanth S. *Vibrio furnissii*, an emerging pathogen causing acute gastroenteritis: a Case Report, JMM Case Rep. 2017; 4(9): e005111.

Bekemeier H, Giessler AJ. Thrombosis induction by different carrageenans in rats and mice, Naturwissenschaften 1987; 74(7): 345-346.

Bello CA, Hermogenes AL, Magalhaes A, Veiga SS, Gremski LH, Richardson M, Sanchez EF. Isolation and biochemical characterization of a fibrinolytic proteinase from *Bothrops leucurus* (white-tailed jararaca) snake venom, Biochimie. 2006; 88(2): 189-200.

Boulaftali Y, Adam F, Venisse L, Ollivier V, Richard B, Taieb S, Monard D, Favier R, Alessi MC, Bryckaert M, Arocas V, Jandrot-Perrus M, Bouton MC. Anticoagulant and antithrombotic properties of platelet protease nexin-1, Blood 2010; 115(1): 97-106.

Bradford MM. A rapid and sensitive method for the quantitation of microgram quantities of protein utilizing the principle of protein-dye binding, Anal. Biochem. 1976; 72(1): 248-254.

Brenner DJ, Hickman-Brenner FW, Lee JV, Steigerwalt AG, Fanning GR, Hollis DG, Farmer JJ 3rd, Weaver RE, Joseph SW, Seidler RJ. Vibrio furnissii (formerly aerogenic biogroup of Vibrio fluvialis), a new species isolated from human feces and the environment, J. Clin Microbiol. 1983; 18(4): 816-824.

Carter AM, Cymbalista CM, Spector TD, Grant PJ. Heritability of clot formation, morphology, and lysis, Arterioscler Thromb. Vasc. Biol. 2007; 27(12): 2783-2789.

Chang AK, Kim HY, Park JE, Acharya P, Park IS, Yoon SM, You HJ, Hahm KS, Park JK, Lee JS. Vibrio vulnificus secretes a broad-specificity

metalloprotease capable of interfering with blood homeostasis through prothrombin activation and fibrinolysis, J. Bacteriol. 2005; 187(20): 6909-6916.

Chang AK, Park JW, Lee EH, Lee JS. The N-terminal propeptide of *Vibrio vulnificus* extracellular metalloprotease is both an inhibitor of and a substrate for the enzyme, J. Bacteriol. 2007; 189(19): 6832-6838.

Choi JH, Sapkota K, Kim S, Kim SJ. Starase: A bi-functional fibrinolytic protease from hepatic caeca of *Asterina pectinifera* displays antithrombotic potential, Biochimie. 2014; 105: 45-57.

Collen D, Lijnen HR. Tissue plasminogen activator: mechanism of action and thrombolytic properties, Haemostasis 1986; 16(Suppl. 4): 26-34.

Derber C, Coudron P, Tarr C, Gladney L, Turnsek M, Shankaran S, Wong E. *Vibrio furnissii*: an unusual cause of bacteremia and skin lesions after ingestion of seafood, J. Clin. Microbiol. 2011; 49(6): 2348-2349.

De-Simone S, Netto C, Antunes OAC, Alencastro R, Silva F. Biochemical and molecular modeling analysis of the ability of two *p*-aminobenzamidine-based sorbents to selectively purify serine proteases (fibrinogenases) from snake venoms, J. Chromatogr. B. Analyt. Technol. Biomed. Life Sci. 2005; 822(1-2): 1-9.

Ghosh M, Pulicherla KK, Rekha VPB, Venkat Rao G, Sambasiva Rao KRS. A review on successive generations of streptokinase based thrombolytic agents, Int. J. Pharm. Pharm. Sci. 2012; 4(Suppl. 3): 38-42.

Giubergia S, Phippen C, Gotfredsen CH, Nielsen KF, Gram L. Influence of niche-specific nutrients on secondary metabolism in *Vibrionaceae,* Appl. Environ. Microbiol. 2016; 82(13): 4035-4044.

Goldhaber SZ, and Bounameaux H. Thrombolytic therapy in pulmonary embolism, Semin. Vasc. Med. 2001; 01(2): 213-220

Hagimori M, Kamiya S, Yamaguchi Y, Arakawa M. Improving frequency of thrombosis by altering blood flow in the carrageenan-induced rat tail

thrombosis model, Pharmacol. Res. 2009; 60(4): 320-323.

Hida S, Miura N N, Adachi Y, & Ohno N. Influence of arginine deimination on antigenicity of fibrinogen, J. Autoimmun. 2004; 23(2): 141-150.

Hirose J, Iwamoto H, Nagao I, Enmyo K, Sugao H, Kanemitu N, Ikeda K, Takeda M, Inoue M, Ikeda T, Masuura F, Fukasawa KM, Fukasawa K. Characterization of the metal-substituted dipeptidyl peptidase III (rat liver), Biochemistry 2001; 40(39): 11860-11865.

Hooper NM. Families of zinc metalloproteases, FEBS. Lett. 1994; 354(1): 1-6.

Huber-Lang, M, Sarma JV, Zetoune FS, Rittirsch D, Neff TA, Mcguire SR, Lambris JD, Warner RL, Flierl MA, Hoesel LM, Gebhard F, Younger JG, Drouin SM, Wetsel RA. & Ward PA. Generation of C5a in the absence of C3: a new complement activation pathway. Nature Medicine 2006; 12: 682 –687.

Jacquemin M, Vanlinthout I, Van Horenbeeck I, Debasse M, Toelen J, Schoeters J, Lavend'homme, Freson K, Peerlinck K. The amplitude of coagulation curves from thrombin time tests allows dysfibrinogenemia caused by the common mutation FGG-Arg301 to be distinguished from hypofibrinogenemia, Int. J. Lab. Hematol. 2017; 39(3): 301-307.

Janeway CA Jr, Travers P, Walport M, Shlomchik MJ. Immunobiology: The Immune System in Health and Disease. 5th edition. New York: Garland Science; 2001.

Kaiser M, Jacobson M, Andersen PH, Baekbo P, Ceron JJ, Dahl J, Escribano D, Jacobsen S. Inflammatory markers before and after farrowing in healthy sows and in sows affected with postpartum dysgalactia syndrome, BMC. Vet. Res. 2018; 14(83): 1-15

Keragala CB, Draxler DF, McQuilten ZK. and Medcalf RL. Haemostasis and innate immunity – a complementary relationship, Br. J. Haematol. 2018; 180: 782-798.

Kostylev M, Otwell AE, Richardson RE, Suzuki Y. Cloning should be simple:

Escherichia coli DH5 alpha-mediated assembly of multiple DNA fragments with short end homologies, PLoS One 2015; 10(9): e0137466.

Kothary MH, McCardell BA, Frazar CD, Deer D, Tall BD. Characterization of the zinc-containing metalloprotease encoded by *zpx* and development of a species-specific detection method for *Enterobacter sakazakii,* Appl. Environ. Microbiol. 2007; 73(13): 4142-4151.

Kuenzi MJ, Sherwood OD. Immunohistochemical localization of specific relaxin-binding cells in the cervix, mammary glands, and nipples of pregnant rats, Endocrinology 1995; 136(4): 1367-1373.

Kwon JY, Chang AK, Park JE, Shin SY, Yoon SM, Lee JS. Vibrio extracellular protease with prothrombin activation and fibrinolytic activities, Int. J. Mol. Med. 2007; 19(1): 157-163.

Leonardi A, Gubensek F, Krizaj I. Purification and characterisation of two hemorrhagic metalloproteinases from the venom of the long-nosed viper, *Vipera ammodytes ammodytes,* Toxicon 2002; 40(1): 55-62.

Li B, Fu C, Ma G, Fan Q, Yao Y. Photoacoustic imaging: a novel tool for detecting carotid artery thrombosis in mice, J. Vasc. Res. 2017; 54(4): 217-225.

Lippi G, Mattiuzzi C, Favaloro EJ. Novel and emerging therapies: thrombus-targeted fibrinolysis, Semin. Thromb. Hemost. 2013; 39(1): 48-58.

Liu Y, Jennings NL, Dart AM, Du XJ. Standardizing a simpler, more sensitive and accurate tail bleeding assay in mice, World J. Exp. Med. 2012; 2(2): 30-36.

Lux TM, Lee R, Love J. Complete genome sequence of a free-living *Vibrio furnissii* sp. nov. strain (NCTC 11218), J. Bacteriol. 2011; 193(6): 1487-1488.

Ma N, Liu XW, Yang YJ, Li JY, Mohamed I, Liu GR, Zhang JY. Preventive effect of aspirin eugenol ester on thrombosis in κ-carrageenan-induced rat tail thrombosis model, PLoS One 2015; 10(7): e0133125.

Majumdar S, Chattopadhyay P, Mukherjee AK. *In vivo* anticoagulant and thrombolytic activities of a fibrinolytic serine protease (Brevithrombolase) with the *k*-carrageenan-induced rat tail thrombosis model, Clin. Appl. Thromb. Hemostasis 2016; 22(6): 594-598.

Matsubara K, Hori K, Matsuura Y, Miyazawa K. Purification and characterization of a fibrinolytic enzyme and identification of fibrinogen clotting enzyme in a marine green alga, *Codium divaricatum,* Comp. Biochem. Physiol. B. Biochem. Mol. Biol. 2000; 125(1): 137-143.

Matsushima A, Shioya K, Kobayashi M, Kodera Y, Inada Y. Activation of fibrinolysis with the protease from *Dermatophagoides farinae,* Thromb. Haemost. 1993; 70(3): 545.

Miyoshi S, Wakae H, Tomochika K, Shinoda S. Functional domains of a zinc metalloprotease from *Vibrio vulnificus,* J. Bacteriol. 1997; 179(23): 7606-7609.

Pancioli AM. Combination pharmacotherapy for achievement and maintenance of vascular patency, Stroke 2009; 40(Suppl. 3): S99-102.

Park JE, Kim HI, Park JW, Park JK, Lee JS. Cloning and biochemical characterization of Staphylococcus aureus type IA DNA topoisomerase comprised of distinct five domains, Arch. Biochem. Biophys. 2011; 508(1): 78-86.

Park JE, Park JW, Lee W, Lee JS. Pleiotropic effects of a vibrio extracellular protease on the activation of contact system. Biochem. Biophys. Res. Commun. 2014; 450(2): 1099-1103.

Park JW, Park JE, Choi HK, Jung TW, Yoon SM, Lee JS. Purification and characterization of three thermostable alkaline fibrinolytic serine proteases from the polychaete *Cirriformia tentaculata,* Process Biochem. 2013; 48(5): 979-987.

Park JW, Park JE, Park JK, Lee JS. Purification and biochemical characterization of a novel glutamyl endopeptidase secreted by a clinical

isolate of *Staphylococcus aureus,* Int. J. Mol. Med. 2011; 27(5): 637-645.

Park JY, Park JE, Park JW, Yoon SM, Lee JS. Purification and characterization of a novel alkaline serine protease secreted by *Vibrio metschnikovii,* Int. J. Mol. Med. 2012; 29(2): 263-268.

Sakamoto S, Putalun W, Vimolmangkang S, Phoolcharoen W, Shoyama Y, Tanaka H, Morimoto S. Enzyme-linked immunosorbent assay for the quantitative/qualitative analysis of plant secondary metabolites, J. Nat. Med. 2018; 72(1): 32-42.

Sakuragawa N, Takahashi K, Koide T. The effects of trypsin and plasmin on coagulation fibrinolytic factors, Acta. Med. Biol. 1975; 23(2): 91-102.

Stepanenko AA, Dmitrenko VV. Pitfalls of the MTT assay: direct and off-target effects of inhibitors can result in over/underestimation of cell viability, Gene 2015; 574(2): 193-203.

Swenson S, Markland FS, Jr. Snake venom fibrin(ogen)olytic enzymes, Toxicon 2005; 45(8): 1021-1039.

Tough J. Thrombolytic therapy in acute myocardial infarction, Nurs. Stand. 2005; 19(37): 55-64.

Laemmli UK. Cleavage of structural proteins during the assembly of the head of bacteriophage T4, Nature 1970; 227(5259): 680-685.

Verstraete M. Third generation thrombolytic drugs. Am. J. Med. 2000; 109(1): 52-58.

Wang X, Cheng Q, Xu L, Feuerstein GZ, Hsu MY, Smith PL, Seiffert DA, Schumaher WA, Ogletree ML, Gailani D. Effects of factor IX or factor XI deficiency on ferric chloride-induced carotid artery occlusion in mice, J. Thromb. Haemost. 2005; 3(4): 695-702.

You WK, Jang YJ, Chung KH, Jeon OH, Kim DS. Functional roles of the two distinct domains of halysase, a snake venom metalloprotease, to inhibit human platelet aggregation. Biochem. Biophys, Res. Commun. 2006; 339(3): 964-970.

Yu B, Zhang G, Jin L, Zhang B, Yan D, Yang H, Ye Z, Ma T. Inhibition of PAI-1 activity by toddalolactone as a mechanism for promoting blood circulation and removing stasis by chinese herb *Zanthoxylum nitidum* var. *tomentosum,* Front. Pharmacol. 2017; 8(Article 489): 1-11.

Zhu Z, Sun D, Davidson VL. Localization of periplasmic redox proteins of *Alcaligenes faecalis* by a modified general method for fractionating gram-negative bacteria, J. Bacteriol. 1999; 181(20): 6540-6542.